

Journal of Visualized Experiments

Construction of a wireless-enabled endoscopically implantable sensor for pH monitoring with zero-bias Schottky diode-based receiver --Manuscript Draft--

Article Type:	Methods Article - JoVE Produced Video
Manuscript Number:	JoVE62864R1
Full Title:	Construction of a wireless-enabled endoscopically implantable sensor for pH monitoring with zero-bias Schottky diode-based receiver
Corresponding Author:	Marek Novák Charles University Third Faculty of Medicine: Univerzita Karlova 3 lekarska fakulta Prague, Prague CZECH REPUBLIC
Corresponding Author's Institution:	Charles University Third Faculty of Medicine: Univerzita Karlova 3 lekarska fakulta
Corresponding Author E-Mail:	marek.novak@lf3.cuni.cz
Order of Authors:	Marek Novák Jozef Rosina Robert Gürlich Ivana Cibulková Jan Hajer
Additional Information:	
Question	Response
Please specify the section of the submitted manuscript.	Bioengineering
Please indicate whether this article will be Standard Access or Open Access.	Standard Access (\$1400)
Please indicate the city, state/province, and country where this article will be filmed . Please do not use abbreviations.	Prague, capital city of the Czech Republic
Please confirm that you have read and agree to the terms and conditions of the author license agreement that applies below:	I agree to the Author License Agreement
Please provide any comments to the journal here.	
Please confirm that you have read and agree to the terms and conditions of the video release that applies below:	I agree to the Video Release

TITLE:

Construction of a Wireless-Enabled Endoscopically Implantable Sensor for pH Monitoring with Zero-Bias Schottky Diode-based Receiver

AUTHORS AND AFFILIATIONS:

Marek Novák^{*1}, Jozef Rosina¹, Robert Gürlich², Ivana Cibulková³, Jan Hajer³

¹Department of Medical Biophysics and Medical Informatics, Third Faculty of Medicine, Charles University, Prague, 100 00, Czech Republic

²Department of General Surgery, Third Faculty of Medicine, Charles University, University Hospital Královské Vinohrady, Prague, 100 34, Czech Republic

³Department of Internal Medicine, Third Faculty of Medicine, Charles University, University Hospital Královské Vinohrady, Prague, 100 34, Czech Republic

Email addresses of co-authors:

Marek Novák (marek.novak@lf3.cuni.cz)

Jozef Rosina (jozef.rosina@lf3.cuni.cz)

Robert Gürlich (robert.gurlich@fnkv.cz)

Ivana Cibulková (ivana.cibulkova@fnkv.cz)

Jan Hajer (jan.hajer@fnkv.cz)

*Corresponding author

Marek Novák (marek.novak@lf3.cuni.cz)

SUMMARY:

The manuscript presents a miniature implantable pH sensor with ASK modulated wireless output together with a fully passive receiver circuit based on zero-bias Schottky diodes. This solution can be used as a basis in the development of *in vivo* calibrated electrostimulation therapy devices and for ambulatory pH monitoring.

ABSTRACT:

Ambulatory pH monitoring of pathological reflux is an opportunity to observe the relationship between symptoms and exposure of the esophagus to acidic or non-acidic refluxate. This paper describes a method for the development, manufacturing, and implantation of a miniature wireless-enabled pH sensor. The sensor is designed to be implanted endoscopically with a single hemostatic clip. A fully passive rectenna-based receiver based on a zero-bias Schottky diode is also constructed and tested. To construct the device, a two-layer printed circuit board and off-the-shelf components were used. A miniature microcontroller with integrated analog peripherals is used as an analog front end for the ion-sensitive field-effect transistor (ISFET) sensor and to generate a digital signal which is transmitted with an amplitude shift keying transmitter chip. The device is powered by two primary alkaline cells. The implantable device has a total volume of 0.6 cm³ and a weight of 1.2 grams, and its performance was verified in an *ex vivo* model (porcine esophagus and stomach). Next, a small footprint passive rectenna-based receiver which can be easily integrated either into an external receiver or the implantable neurostimulator, was

constructed and proven to receive the RF signal from the implant when in proximity (20 cm) to it. The small size of the sensor provides continuous pH monitoring with minimal obstruction of the esophagus. The sensor could be used in routine clinical practice for 24/96 h esophageal pH monitoring without the need to insert a nasal catheter. The “zero-power” nature of the receiver also enables the use of the sensor for automatic *in-vivo* calibration of miniature lower esophageal sphincter neurostimulation devices. An active sensor-based control enables the development of advanced algorithms to minimize the used energy to achieve a desirable clinical outcome. One of the examples of such an algorithm would be a closed-loop system for on-demand neurostimulation therapy of gastroesophageal reflux disease (GERD).

INTRODUCTION:

The Montreal Consensus defines gastroesophageal reflux disease (GERD) as “a condition that develops when refluxing the contents of the stomach causes unpleasant symptoms and/or complications”. It may be associated with other specific complications such as esophageal strictures, Barrett’s esophagus, or esophageal adenocarcinoma. GERD affects approximately 20% of the adult population, mainly in countries with high economic status¹.

Ambulatory pH monitoring of pathological reflux (acid exposure time of more than 6%) allows us to distinguish the relationship between symptoms and acidic or non-acidic gastroesophageal reflux^{2,3}. In patients unresponsive to PPI (proton pump inhibitor) therapy, pH monitoring can answer whether it is pathological gastroesophageal reflux and why the patient does not respond to standard PPI therapy. Various pH and impedance monitoring options are currently offered. One of the newer possibilities is wireless monitoring using implantable devices^{4,5}.

GERD is associated with lower esophageal sphincter (LES) disorder, where the contractions shown during esophageal manometry are not pathological but have a reduced amplitude in long-term GERD. LES consists of smooth muscle and maintains tonic contractions due to myogenic and neurogenic factors. It relaxes due to vagal-mediated inhibition involving nitric oxide as a neurotransmitter⁶.

Electrical stimulation with two pairs of electrodes was proven to increase the contraction time of the LES in a canine reflux model⁷. The relaxation of the LES including the residual pressure during swallowing was not affected by both low and high frequency stimulation. High-frequency stimulation is an obvious choice because it requires less power and extends the battery life.

Although electrostimulation treatment (ET) of the lower esophageal sphincter is a relatively new concept in the treatment of patients with GERD, this therapy was shown to be safe and effective. This form of treatment has been shown to provide significant and lasting relief from the symptoms of GERD while eliminating the need for PPI treatment and reducing esophageal acid exposure^{8–10}.

The current state-of-the-art pH sensor for diagnostics of GERD is the Bravo device^{11,12}. At an estimated volume of 1.7 cm³, it can be implanted directly into the esophagus with or without visual endoscopic feedback and provides 24 h+ monitoring of pH in the esophagus.

89
90 Considering that electrostimulation therapy is one of the most promising alternatives for treating
91 GERD not responding to standard therapy^{8,13}, it makes sense to provide the data from the pH
92 sensor to the neurostimulator. The recent research shows a clear path to future development in
93 this field which will lead to rigid all-in-one implantable devices which will reside at the site of
94 neurostimulation^{14,15}. For this purpose, the ISFET (ion-sensitive field-effect transistor) is one of
95 the best types of sensors because of its miniature nature, the possibility of on-chip integration of
96 a reference electrode (gold in this case), and sufficiently high sensitivity. On silicon, the ISFET
97 resembles the structure of a standard MOSFET (Metal Oxide Semiconductor Field Effect
98 Transistor). However, the gate, normally connected to an electrical terminal, is replaced by a
99 layer of active material in direct contact with the surrounding environment. In the case of pH-
100 sensitive ISFETs, this layer is formed by silicon nitride (Si_3N_4)¹⁶.

101
102 The main disadvantage of implantable devices is the inherent limitation of the battery size, which
103 may lead to a reduced lifetime of these devices or motivate the manufacturers to develop
104 advanced algorithms that will deliver the required effect at a lower energy cost. One of the
105 examples of such an algorithm would be a closed-loop system for on-demand neurostimulation
106 therapy of GERD. Similar to continuous glucose meters (CGM) + insulin pump systems¹⁷, such a
107 system would employ an esophageal pH sensor or another sensor to detect the current pressure
108 of the lower esophageal sphincter together with a neurostimulation unit.

109
110 The response to the neurostimulation therapy and the requirements for neurostimulation
111 patterns can be individual¹³. Thus, it is important to develop independent sensors that could be
112 used either for diagnosis and characterization of the dysfunction or to actively participate in
113 calibrating the neurostimulation system according to the individual requirements of the
114 patients¹⁸. These sensors should be as small as possible to not affect the normal functionality of
115 the organ.

116
117 This manuscript describes a method of design and fabrication of an ISFET based pH sensor with
118 amplitude-shift keying (ASK) transmitter and a small footprint passive rectenna-based receiver.
119 Based on the simple architecture of the solution, the pH data can be received by an external
120 receiver or even the implantable neurostimulator without any significant volume or power
121 penalty. The ASK modulation is chosen because of the nature of the passive receiver, which is
122 only capable of detection of received RF signal power (often called “received signal strength”).
123 The schematic diagram, which is embedded as Supplementary material, shows the construction
124 of the device. It is powered directly from two AG1 alkaline batteries, which provide a voltage
125 between 2.0–3.0 V (based on the state of charge). The batteries power the internal
126 microcontroller, which utilizes its ADC (analog-to-digital converter), DAC (digital-to-analog
127 converter), internal operation amplifier, and FVR (fixed-voltage reference) peripherals to bias the
128 ISFET pH sensor. The resulting “gate” voltage (the gold reference electrode) is proportional to
129 the pH of the surrounding environment. A stable I_{ds} current is provided by a low-side R2 sensing
130 resistor. The source of the ISFET sensor is connected to the non-inverting input of the operational
131 amplifier, while the inverting input is connected to the output voltage of the DAC module set to
132 960 mV. The output of the operational amplifier is connected to the drain pin of the ISFET. This

operational amplifier regulates the drain voltage so that the voltage difference on the R2 resistor is always 960 mV; thus, a constant bias current of 29 μ A flows through the ISFET (when in normal operation). The gate voltage is then measured with an ADC. The microcontroller then powers on the RF transmitter via one of the GPIO (general purpose input/output) pins and transmits the sequence. The RF transmitter circuit involves a crystal and matching network which matches the output to 50 Ω impedance.

For the experiments demonstrated here, we used a pig stomach with a long section of the esophagus mounted in a standardized plastic model. This is a commonly used model for practicing endoscopic techniques such as ESD (endoscopic submucosal dissection), POEM (oral endoscopic myotomy), endoscopic mucosal resection (EMR), hemostasis, etc. Concerning the closest possible anatomical parameters approaching human organs, we used the stomach and esophagus of pigs weighing 40–50 kg.

PROTOCOL:

No living animals were involved in this study. The experiment was performed on an *ex vivo* model consisting of a porcine esophagus and stomach. The stomach and esophagus were purchased from a local butchery as their standard product. This procedure is in accordance with Czech laws, and we prefer it because of the “3R” principle (Replacement, Reduction, and Refinement).

1. Fabrication of the pH sensor assembly

NOTE: Observe precautions for handling electrostatic discharge (ESD) sensitive components throughout the fabrication of the pH sensor assembly. Be careful when working with the soldering iron.

1.1. Place the ISFET pH sensor mounted on a printed circuit board (PCB) on a flat surface. Locate the solderable contacts.

1.2. Trim the solderable contacts, so their length is no longer than 3 mm.

1.3. Solder a 15 mm section of fluorinated ethylene propylene (FEP) coated cable to the solderable electrodes of the pH sensor. Do not mechanically or chemically clean the bare die assembly. Try to avoid contamination of the die and PCB with flux during soldering.

1.4. Inspect the pH sensor-cable assembly under a microscope for open circuits and shorts. Then, check the shorts with an open-short tester. A correctly prepared assembly at this stage is shown in **Figure 1**.

1.5. Clean the pH sensor assembly in an ultrasonic cleaner for 5 min at 70 °C in a 5% solution of flux remover in water. The optimum range of ultrasound power is 50–100 W/l. Do not exceed 100 W/l.

1.6. Rinse the pH sensor assembly in technical grade isopropyl alcohol for at least 3 min and let it dry in an oven at 80 °C for 15 min.

1.7. Place all pH sensors on a flat surface (in case multiple are prepared simultaneously) before proceeding to the next step.

1.8. Mix an appropriate amount of two-part epoxy for encapsulation of the soldered electrodes. Use a minimum of 2 mL to allow thorough mixing. Use black opaque epoxy to allow for inspection later – parts of the sensor exposed to the environment will be seen easier as they will not have opaque epoxy on them

1.9. Transfer the mixed epoxy to a 1 mL syringe with a 0.5 mm flat end needle.

1.10. Coat the soldering area of pH sensors with epoxy. Make sure to coat the whole area of PCB electrodes and the exposed wire.

1.11. Let the epoxy cure either at room or elevated temperature (80 °C max), for this study 50 °C was used with the epoxy listed in the **Table of Materials**.

1.12. Inspect the coated area under a microscope. If any uncoated metal parts (either PCB electrode or wire) are exposed, repeat steps 1.8–1.11 until there are no visual signs of uncoated metal.

1.13. Trim the wires to the length and angle shown in **Figure 2**. Coat the ends with solder to avoid fraying.

2. Fabrication of the electronic assembly

NOTE: Observe precautions for handling ESD-sensitive components throughout the fabrication of the electronics. Be careful when working with the soldering iron and hot-air gun.

2.1. Place the PCB (manufactured based on the supplementary files “pcb1.zip” and schematic diagram “schematic.png”) on a flat surface, components side up.

2.2. Apply solder paste to all the exposed gold-plated pads.

2.3. Place all passive and active components using tweezers according to **Figure 3** and the **Table of Materials**.

2.4. Heat the PCB with the hot air gun to solder the components. Heat the PCB gradually to 150 °C for 2 min to expel residual water from the packages and activate the flux in the solder paste. Then, heat the PCB to 260 °C to solder the components. Let the PCB cool to room temperature, do not move it during the whole soldering process.

2.5. After soldering and cooling down to room temperature, inspect the PCB under a microscope to verify the correct placement of all the components and shorts. If no shorts or incorrect component placement is observed, skip step 2.6.

2.6. Repair any shorts or incorrect component placement with a soldering gun or hot air gun. Go to step 2.5.

2.7. Solder 5 wires to the components (power and programming leads) as shown in **Figure 4**.

2.8. To connect the PCB to the programmer, connect the wires soldered in step 2.7. to the connector of the programmer.

2.9. Program firmware (see **Representative Results** for a detailed explanation of which file to use) to the microcontroller. Use the previously described procedure to set up the programming software¹⁹. Set the programmer to power the device with a voltage of approximately 2.5 V. Desolder the 5 wires after programming.

2.10. Place the PCB on a flat surface, component side up. Solder the AWG38 copper antenna wire (length of 3 cm) as shown in **Figure 5** and wrap it around the edge of the PCB. Fix the antenna wire to the edge of the PCB with a cyanoacrylate adhesive. Solder the other two wire jumpers with SWG38 copper wire as shown in **Figure 5**. Avoid electrical contact with other components.

2.11. Put the PCB on a flat surface, component side down.

2.12. Solder two battery holders to the opposite part of PCB, as shown in **Figure 6**.

2.13. Solder the pH sensor assembly to the terminals on the PCB, as shown in **Figure 7**.

2.14. Insert two AG1 batteries into the battery holders.

NOTE: Do not proceed with this step and next steps in this section earlier than 24 h before testing and endoscopic implantation of the sensor.

2.15. Prepare an appropriate amount of epoxy as described in step 1.8. for encapsulation of the device.

2.16. Encapsulate the device with the epoxy using the same procedure described in step 1.9 (syringe with a needle). Let the epoxy cure at room temperature or slightly elevated temperature (do not exceed 50 °C because of the presence of batteries). See **Figure 8** for the correct encapsulation results.

2.17. Create a titanium wire hook according to **Figure 9**.

NOTE: Titanium (Grade II) was chosen because of its biocompatibility and track record of use in

implantable medical devices. Stainless steel may be used, too. However, the type and heat treatment must be chosen carefully as some stainless steel types are very brittle.

2.18. Attach the wire hook to the device with a drop of fast-curing epoxy (see **Figure 10**) and let it cure at room temperature or slightly elevated temperature (50 °C maximum). The pH sensor is located on the bottom left side of the implantable device.

2.19. The sensor becomes activated 24 h after the insertion of the batteries. Meanwhile, proceed with step 3.

NOTE: Pause the protocol now if completion of step 3 within 24 h after insertion of the batteries is possible.

3. Fabrication of passive rectenna receiver

3.1. Place the PCB (manufactured based on the supplementary file “pcb2.zip”). for the rectenna on a flat surface.

3.2. Solder the components using the solder paste method described in steps 2.2–2.6 or use a soldering gun according to **Figure 11A**.

NOTE: If the experimenter decides to manufacture the rectenna receiver again (it was previously manufactured and matched) or does not want to proceed with receiver matching, use the values of the components previously determined by the experimenter or provided in **Figure 11B** and skip steps 3.5–3.7.

3.3. Solder the SMA connector to the PCB.

3.4. Inspect the PCB under a microscope. If any shorts or incorrect component placement is observed, fix the issues.

3.5. Attach a vector network analyzer input to the SMA connector.

3.6. Record the S11 Smith chart of the rectenna from 300–500 MHz with 1 kHz resolution bandwidth. Observe the response and record the impedance at 431.7 MHz. Use an impedance matching calculator software to determine the values of matching components. The sample Smith chart is shown in **Figure 12A**.

3.7. Solder the impedance matching components and inspect under a microscope for short circuits and component placement.

3.8. Measure with spectrum analyzer again and confirm that the voltage standing wave ratio (VSWR) is under 3 between 300–500 MHz (inside the outer cyan circle shown in **Figure 12B**). If not, either repeat with different matching components or continue with the reduced

performance of the rectenna in mind.

3.9. Connect the 433 MHz band antenna to the SMA connector. Connect an oscilloscope to the rectenna output.

3.10. Set the oscilloscope to single-channel operation, rolling time base, DC mode, 500 ms/div time base, and 5 mV/div voltage scale.

4. Testing of the device

NOTE: The following steps require the use of chemicals. Study the material safety data sheets of the chemicals beforehand and use proper protective equipment and common lab practices when manipulating them.

4.1. Inspect the output of the sensor by observing the signal shown on the oscilloscope. The sample output is shown in **Figure 13,14**. The device will be active after 24 h past the insertion of the batteries. The period of transmitting the output of the pH sensor varies depending on the file which was programmed to the microcontroller (see **Representative Results** for a detailed explanation).

4.2. Prepare 2% hydrochloric acid solution (use caution when handling hydrochloric acid). Prepare 100 mM buffer solutions of pH 4 (potassium hydrogen phthalate/hydrochloric acid), pH 7 (potassium dihydrogen phosphate/sodium hydroxide), and pH 10 (sodium carbonate/sodium hydrogen carbonate) using standard laboratory procedures and mark the beakers.

4.3. Verify the pH of all four beakers using a calibrated pH meter. Adjust if needed.

4.4. Submerge the capsule in every beaker and record at least 3 samples. Measure the period between the second and third pulse and fill it in the provided spreadsheet (**Supplemental File 1**). Determine the calibration coefficients for the pH sensor using the spreadsheet.

4.5. After calibration, measure the time between the second and the third pulse and input it into the spreadsheet to determine the pH of the solution to which the pH sensor is exposed.

5. Endoscopic implantation of the sensor

5.1. Prepare an *ex vivo* endoscopic porcine model made up of the stomach and a long segment of the esophagus.

5.2. Grasp the sensor externally with a hemostatic clip, as shown in **Figure 15** and **Figure 16**.

5.3. Insert the endoscope with the sensor in the clip in the standard way into the model.

5.4. Position the clip with the sensor close to the lower esophageal sphincter.

5.5. Rotate the endoscope against the esophageal wall, open the clip and then push toward the esophageal wall. Close the clip and release the clip. The sensor will remain attached to the esophageal wall at the desired location, as shown in **Figure 17D** and **Figure 17E**.

5.6. Extract the endoscope.

6. Experiment after implantation

NOTE: The following steps require the use of chemicals. Study the material safety data sheets of the chemicals beforehand and use proper protective equipment and common lab practices when manipulating them.

6.1. Place the receiver within 10 cm (maximum) of the implanted sensor.

6.2. Inject 50 mL of the solutions with various pH values into the esophagus, as shown in **Figure 18**, and observe the changes in the sensor's response. Retract the endoscope after every injection and read the value no earlier than 30 s after injection. Wash the esophagus with 100 mL of deionized water between injecting solutions with different pH.

6.3. Use the spreadsheet (**Supplemental File 1**) to calculate the pH measured by the sensor.

REPRESENTATIVE RESULTS:

A device capable of autonomous pH sensing and wireless transmitting of the pH value was successfully constructed, as shown in **Figure 8**. The constructed device is a miniature model; it weighs 1.2 g and has a volume of 0.6 cm³. The approximate dimensions are 18 mm x 8.5 mm x 4.5 mm. As shown in **Figure 15**, **Figure 16**, and **Figure 17**, it can be implanted to the proximity of the lower esophageal sphincter with a single hemostatic clip; no special accessories are needed. A detailed view of a dissected esophagus with the sensor implanted is shown in **Figure 19**.

The passive rectenna receiver has an overall footprint of only 22 mm² even though it is optimized for hand-soldering. When the passive rectenna receiver is put into proximity of the pH sensing device (10 cm) when in an active state (24 h after insertion of batteries until full discharge of the batteries), clear voltage spikes can be observed when the device is transmitting. This is shown in **Figure 13**. The first two short (75 ms) pulses are synchronization pulses. The distance between the end of the second pulse and the beginning of the third pulse is proportional to the V_{gs} voltage of the ISFET subtracted by 800 mV (100 ms = 900 mV, 200 ms = 1000 mV, etc.). This voltage linearly translates to the pH of the environment that the sensor is subjected to.

Based on a simple two-point calibration with pH buffers of pH 4 and pH 10 (**Table 1**), the sensor can return stable and repeatable pH value readings (**Table 2**). A total of four different solutions with known pH were used—pH 0.6 (160 mM solution of hydrochloric acid in the water, mimicking the stomach acid²⁰) and calibration buffers with pH 4, pH 7, and pH 10. The mean error pH values

of the sensor were 0.25 and 0.31 when tested in solutions in beakers and an *ex vivo* model, respectively. The standard deviations of the errors were 0.30 and 0.36, respectively.

When in the proximity of the transmitter (10 cm), the passive rectenna produces a signal with an amplitude of at least tens of millivolts which can be easily detected by a simple comparator or amplified with an ultra-low-power quiescent current operational amplifier. The effect of a mobile phone antenna with an active GSM call has only a minor negative effect on receiving the data from the sensor, as demonstrated in **Figure 14**. The mobile phone transmission peaks can be filtered by a simple passive RC/LC (resistor-capacitor/inductor-capacitor) filter as they form a high-frequency part of the signal (their frequency is generally above 500 Hz).

In one of the devices, a short circuit between all three of the ISFET electrodes was intentionally made to show how the device's behavior changes when the device is incorrectly assembled. In this case, no voltage-pH response is observed, and the gate voltage is equal to the drain voltage, which is the battery pack voltage (2–3.2 V). The AD converter, which is referenced to an internal 2.048 V reference, then returns the highest possible value, which translates to 2048 mV. Noise may cause slight fluctuations in the ADC output.

Two variants of firmware that can be programmed to the device were developed and tested. The first one (firmware_10s.zip) is intended for short-term experiments where the pH value is transmitted every 10 s. This provides more data points for the cost of reduced battery life, which is limited to around 24–30 h. The other one (firmware_1min.zip) is intended for long-term experiments. The pH value is transmitted once per min. The lifetime of the sensor with a lower sampling frequency is around 5–6 days. There is also a version of the firmware (firmware-test.zip), which does not include the 24 h delay. This file can be used for testing the correct functionality of the electronics before encapsulation. Alternatively, the delay can be modified by changing the code and recompiling the project. The delay was implemented to allow for a full cure of the epoxy or a possibility when the device is manufactured at a different site than the endoscopic surgery room. With the introduced delay, the useful operating life of the device is maximized.

FIGURE AND TABLE LEGENDS:

Figure 1: pH sensor assembly before final trimming

Figure 2: pH sensor assembly after final trimming

Figure 3: Placement diagram for the implantable sensor (see **Table of Materials** for component values). Pin 1 is marked as a red dot.

Figure 4: Placement of programming wires

Figure 5: Placement of antenna wire and jumper wires

Figure 6: Placement of battery holders

Figure 7: Soldering of the pH sensor assembly to the electronics

Figure 8: Finished encapsulated sensor. (A) side view, (B) back view

Figure 9: Titanium wire hook

Figure 10: Attachment of the wire hook to the implantable device

Figure 11: Placement diagram for the rectenna. (A) with matching components, (B) without matching components, ready to be matched with a vector network analyzer

Figure 12: Smith chart. (A) unmatched rectenna, (B) matched rectenna

Figure 13: Example response of the rectenna to the incoming data from the sensor

Figure 14: Example response when in the presence of RF noise (nearby phone with an active GSM call). (A) 20 cm between the edge of the phone and receiver, (B) 10 cm between the edge of the phone and receiver, (C) 5 cm between the edge of the phone and receiver

Figure 15: Picture of the endoscope with hemostatic clip and implantable pH sensor

Figure 16: Implantable pH sensor grasped with the hemostatic clip in a cap

Figure 17: Implantation of the sensor. (A) insertion of the endoscope with the implantable pH sensor into the model, (B) place of implantation – 3 cm above the gastroesophageal junction, (C) preparation of the clip placement, (D) the clip was successfully placed, (E) view of the ISFET pH sensor, implanted to the proximity of lower esophageal sphincter

Figure 18: Injection of the pH buffer solution through the endoscope channel

Figure 19: Dissected esophagus of the *ex vivo* model with the implanted sensor

Table 1: Example calibration data

Table 2: Measured data (test with beakers)

Table 3: Measured data (test in an *ex vivo* model)

Supplemental File 1: spreadsheet.xlsx. Spreadsheet for calibrating and processing of the data from the sensor

Supplemental File 2: pcb1.zip. Gerber manufacturing data for the implantable device

Supplemental File 3: pcb2.zip. Gerber manufacturing data for the receiver

Supplemental File 4: firmware_10s.zip. Firmware for the microcontroller with 10 s transmission period

Supplemental File 5: firmware_1min.zip. Firmware for the microcontroller with 1 min transmission period

Supplemental File 6: firmware-test.zip. Firmware for the microcontroller without 24 h pause before activation

Supplemental File 7: Schematic diagram of the electronics

DISCUSSION:

This method is suitable for researchers who work on the development of novel active implantable medical devices. It requires a level of proficiency in the manufacturing of electronic prototypes with surface mount components. The critical steps in the protocol are related to the manufacturing of the electronics, especially populating the PCBs, which is prone to operator error in placement and soldering of small components. Then, correct encapsulation is crucial to prolong the lifetime of the device when exposed to moisture and liquids. The implantation method was designed with simplicity in mind. The risk of perforation of the esophagus or other adverse events during the implantation is minimal. Hemostatic clips are widely used in clinical practice; thus, no special training is needed to perform the implantation.

The device can be easily modified to accompany other sensors with voltage output, i.e., resistive sensors and other ISFET sensors. This gives great flexibility to utilize the whole concept in other areas of research and clinical practice; it is not limited to research of novel methods of treatment of GERD in the case of a pH ISFET sensor.

The constructed device is miniature; it weighs 1.2 g and occupies 60% less volume (0.6 cm³) than the closest commercialized implantable pH sensor. Further miniaturization could be achieved by the integration of the ISFET onto the PCB with wires bonded directly to the PCB. This, however, would significantly increase the barrier of entry in terms of required equipment (it would require at least a manual wire bonder). Thus, a more economically viable alternative with a pre-packaged ISFET sensor by the manufacturer was presented.

As for the power source, silver oxide/alkaline/carbon-zinc 1.5 V cells provide better performance and do simplify the circuit design. The use of primary lithium batteries or Li-Ion batteries in this device form factor could lead to potential problems. Small primary lithium batteries have high output resistance, which would cause significant voltage drops, potentially leading to the brown-out of the microcontroller and RF transmitter. Lithium-ion batteries, on the other hand, are incompatible with 3.3 V microcontrollers (their operating voltage is around 3.0–4.2 V), adding complexity to the circuitry (requirement of a regulator or DC/DC step-down converter). For these reasons, two primary 1.5 V button cells are the best readily available type of battery based on

the availability, operating voltage, and sufficiently low output resistance.

The sensor exhibits good accuracy for esophageal pH monitoring; the mean error of pH in an *ex vivo* model was 0.31 with a standard deviation of 0.36. Despite the washing step with deionized water between each buffer addition, a larger deviation in the *ex vivo* model could have been caused by minor mixing of the different buffer solutions in the esophagus, which may have altered the pH of the solutions. The sensitivity of the used ISFET pH sensor almost follows the Nernstian slope (-58 mV/pH for 25°C) at -51.7 mV/pH . The sensitivity is higher than the reported antimony-based pH sensors for monitoring GERD (-45 mV/pH)²¹.

The delay of 24 h between the insertion of batteries and the start of the wireless transmission routine was introduced to accommodate for encapsulation epoxy curing and instances where the lab for manufacturing of electronics is present at a different location than the endoscopic surgery room. This delay can be altered by modifying the source code and recompiling the firmware.

Depending on the nature of the experiment, which will be done by the researchers, suitable epoxy (cost versus performance) can be chosen. The initial experiments were done with automotive-grade epoxy, which was suitable for initial experiments but not for *ex vivo* experiments from the point of biocompatibility. For survival experiments, a medical-grade epoxy that is ISO10993 compliant for long-term contact with mucous membranes shall be chosen. Also, coatings that improve biocompatibility (e.g., PTFE or parylene) can further reduce the rejection rate of the implant and/or inflammation/irritation of the implantation site.

The fully passive rectenna receiver can be improved by biasing the detector diodes to improve the sensitivity^{22,23}. In case that improved immunity against electromagnetic interference or RF noise is required, the diode detector can be further modified by adding a highly selective band SAW filter between the RF input and diode detector²⁴. If longer-range communication is required, an active ASK receiver (or a software-defined receiver - SDR) can be used. In both cases, the center frequency of the receiver shall be set to 431.73 MHz (frequency of the crystal multiplied by 32 by the PLL in the RF transmitter integrated circuit) and the resolution bandwidth of around 150–250 kHz. The RF output frequency is both voltage and temperature-dependent, and drifts up to 50 kHz from the center frequency were observed during normal operation. The output power in the band can then be monitored and used to decode the pH value according to the protocol. The use of an active receiver is recommended for initial testing. If used inside an implantable device, it comes with an increase in complexity and a major energy penalty. It cannot provide the “zero-power” advantage that the Schottky detector provides.

Today, virtually all active implantable medical devices are not designed with interoperability in mind. Their configuration is done manually by a surgeon or practitioner²⁵ and does not cooperate. The implantable device presented in this method together with a passive rectenna receiver, shows a way to realize seamless data transfer from a disposable sensor to another implantable device. While commercially available RF modules for implantable devices based on the heterodyne concept exist, the receiver mode is very power demanding²⁶. With the presented

solution, no active receiver in the neurostimulator is required; the circuit can be built to be completely passive. The main advantages of taking real-time patient data into account are to improve the efficacy of the therapy and significantly lower the power consumption. For example, in the case of GERD therapy, a pH sensor presented in the manuscript can be implanted above the lower esophageal sphincter after the implantation of the stimulator to automatically adapt the neurostimulation pattern to maximize the effect of the therapy while minimizing the power consumption. As the implantation of the sensor to the inner esophageal wall is prone to dislocation after several days, it makes more sense to design the sensor as a battery-powered one. Thanks to the higher volumetric energy density of primary batteries, the use of a primary power source is superior to a sensor that contains a wireless power receiving circuit, charging coil, and capacitor-based energy storage. The overall efficiency of the wireless charging is also heavily dependent on the spatial orientation of the coils, which would introduce yet another difficulty to the design. Wireless charging provides benefits to the permanently implanted microneurostimulators, i.e., to the submucosa¹⁴. The battery-powered pH sensor provides a possibility to optimize the energy consumption of such a microneurostimulator. Instead of permanent/regular neurostimulation of the sphincter, the pH sensor can show when the stimulation is needed (i.e., primarily at night and/or which hours of the day) and what power output is the lowest possible to achieve sufficient lower esophageal sphincter pressure. These closed-loop or quasi-closed-loop implantable systems can become a promising alternative to current traditional systems, offering smaller implantable devices with less-invasive implantation and improving the treatment's efficacy.

ACKNOWLEDGMENTS:

The authors gratefully acknowledge Charles University (project GA UK No 176119) for supporting this study. This work was supported by the Charles University research program PROGRES Q 28 (Oncology).

DISCLOSURES:

The authors have nothing to declare.

REFERENCES:

1. El-Serag, H. B., Sweet, S., Winchester, C. C., Dent, J. Update on the epidemiology of gastro-oesophageal reflux disease: a systematic review. *Gut*. **63** (6), 871–880 (2014).
2. Gyawali, C. P. et al. Modern diagnosis of GERD: the Lyon Consensus. *Gut*. **67** (7), 1351–1362 (2018).
3. Cesario, S. et al. Diagnosis of GERD in typical and atypical manifestations. *Acta Biomedica*. **89** (5), 33–39 (2018).
4. Sifrim, D., Gyawali, C. P. Prolonged wireless pH monitoring or 24-hour catheter-based pH impedance monitoring: Who, When, and Why? *American Journal of Gastroenterology*. **115** (8), 1150–1152 (2020).
5. Chae, S., Richter, J. E. Wireless 24, 48, and 96 Hour or impedance or oropharyngeal prolonged pH monitoring: Which test, when, and why for GERD? *Current Gastroenterology Reports*. **20** (11), 52 (2018).
6. Furness, J. B., Callaghan, B. P., Rivera, L. R., Cho, H. -J. The enteric nervous system and

gastrointestinal innervation: integrated local and central control. **817**, 39–71 (2014).

7. Sanmiguel, C. P. et al. Effect of electrical stimulation of the LES on LES pressure in a canine model. *American Journal of Physiology-Gastrointestinal and Liver Physiology*. **295** (2), G389–G394 (2008).

8. Rodríguez, L. et al. Electrical stimulation therapy of the lower esophageal sphincter is successful in treating GERD: final results of open-label prospective trial. *Surgical Endoscopy*. **27** (4), 1083–1092 (2013).

9. Rinsma, N. F., Bouvy, N. D., Masclee, A. A. M., Conchillo, J. M. Electrical stimulation therapy for gastroesophageal reflux disease. *Journal of Neurogastroenterology and Motility*. **20** (3), 287–293 (2014).

10. Rodríguez, L. et al. Two-year results of intermittent electrical stimulation of the lower esophageal sphincter treatment of gastroesophageal reflux disease. *Surgery*. **157** (3), 556–567 (2015).

11. Kwiatek, M. A., Pandolfino, J. E. The Bravo™ pH capsule system. *Digestive and Liver Disease*. **40** (3), 156–160 (2008).

12. Karamanolis, G. et al. Bravo 48-hour wireless pH monitoring in patients with non-cardiac chest pain. objective gastroesophageal reflux disease parameters predict the responses to proton pump inhibitors. *Journal of Neurogastroenterology and Motility*. **18** (2), 169–173 (2012).

13. Rodríguez, L. et al. Two-year results of intermittent electrical stimulation of the lower esophageal sphincter treatment of gastroesophageal reflux disease. *Surgery (United States)*. **157** (3), 556–567 (2015).

14. Hajer, J., Novák, M., Rosina, J. Wirelessly powered endoscopically implantable devices into the submucosa as the possible treatment of gastroesophageal reflux disease. *Gastroenterology Research and Practice*. **2019**, 1–7 (2019).

15. Deb, S. et al. Development of innovative techniques for the endoscopic implantation and securing of a novel, wireless, miniature gastrostimulator (with videos). *Gastrointestinal Endoscopy*. **76** (1), 179–184 (2012).

16. Shin, P., Mikolajick, T., Ryssel, H. pH Sensing Properties of ISFETs with LPCVD Silicon Nitride Sensitive-Gate. *The Journal of Electrical Engineering and Information Science*. **2**, 82–87 (1997).

17. Benhamou, P. -Y. et al. Closed-loop insulin delivery in adults with type 1 diabetes in real-life conditions: a 12-week multicentre, open-label randomised controlled crossover trial. *The Lancet Digital Health*. **1** (1), e17–e25 (2019).

18. Nikolic, M. et al. Tailored modern GERD therapy – steps towards the development of an aid to guide personalized anti-reflux surgery. *Scientific Reports*. **9** (1), 19174 (2019).

19. Hajer, J., Novák, M. Autonomous and rechargeable microneurostimulator endoscopically implantable into the submucosa. *Journal of Visualized Experiments: JoVE*. **139**, e57268 (2018).

20. Pavelka, M., Roth, J. *Parietal Cells Of Stomach: Secretion Of Acid. Functional Ultrastructure*. 202–203, Springer, Vienna (2010).

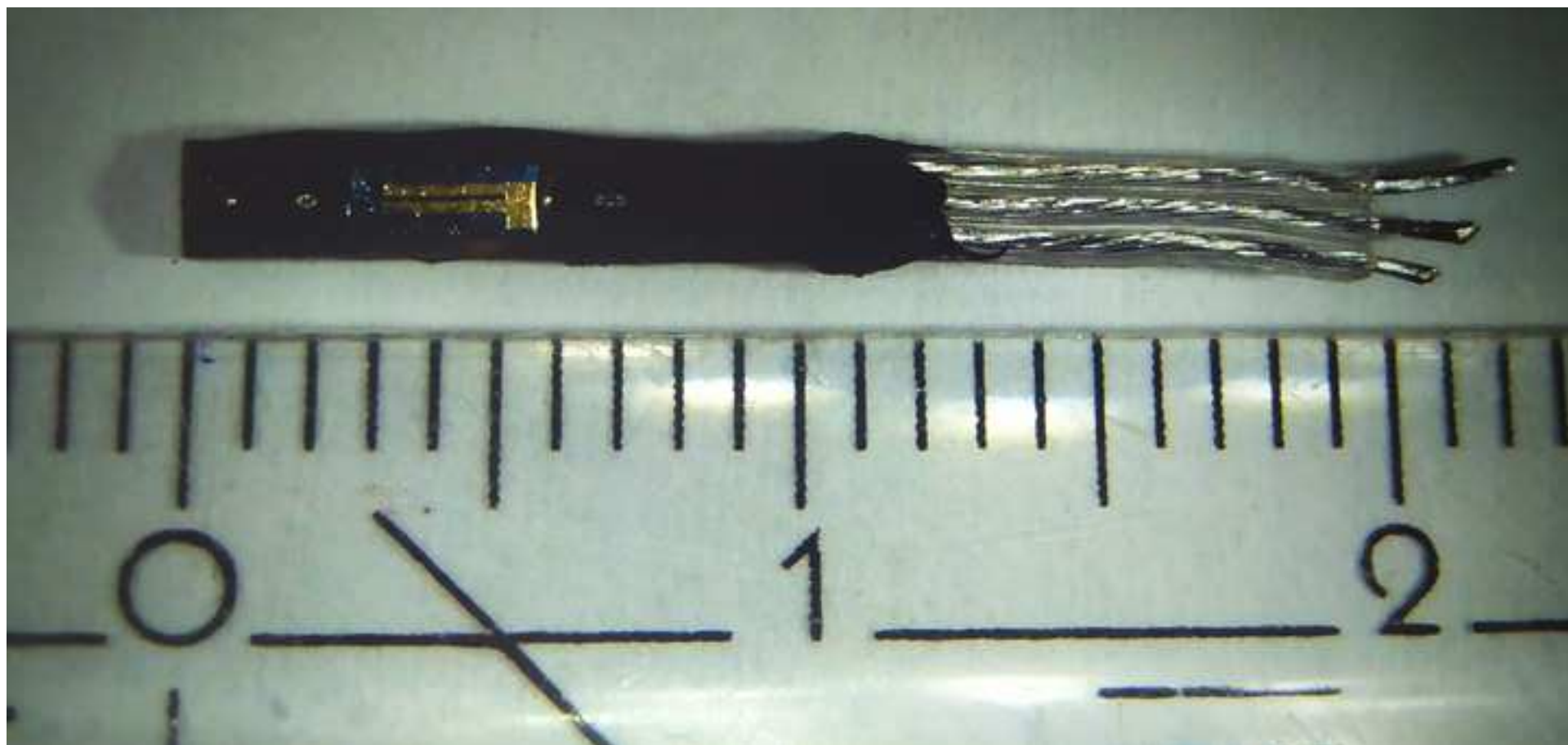
21. Jones, R. D., Neuman, M. R., Sanders, G., Cross, F. S. Miniature antimony pH electrodes for measuring gastroesophageal reflux. *The Annals of Thoracic Surgery*. **33** (5), 491–495 (1982).

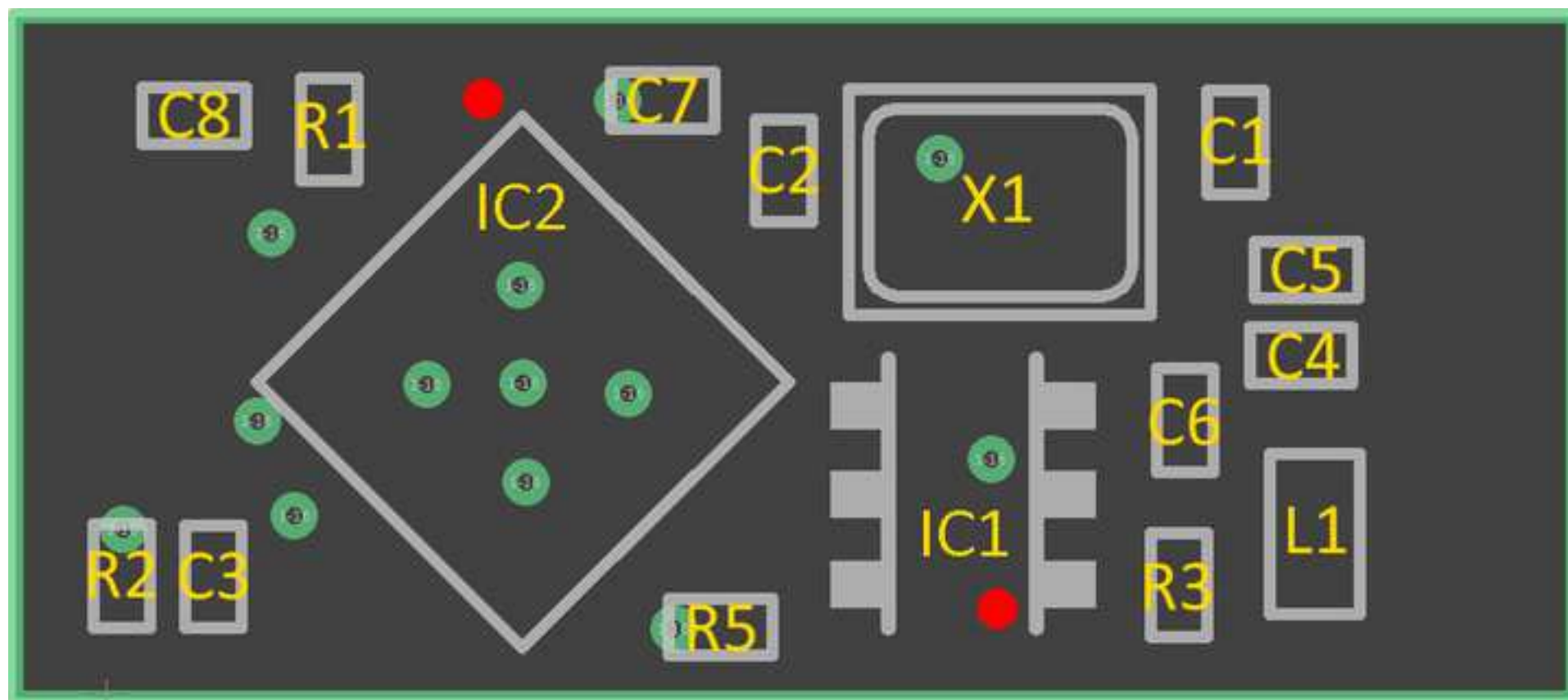
22. Avago technologies designing detectors for RF/ID tags application note 1089. at <<http://docs.avagotech.com/docs/AV02-1577EN>> (2008).

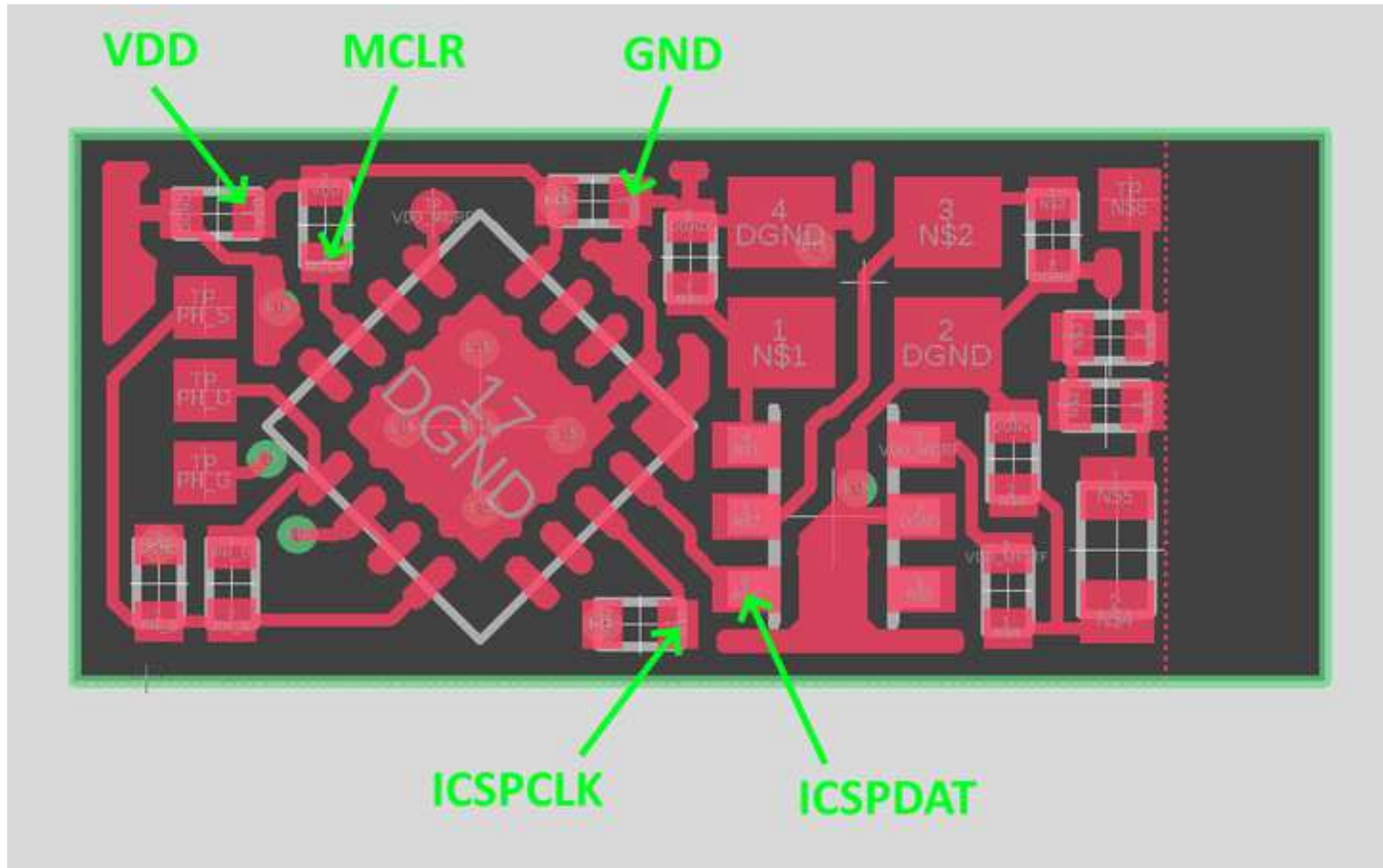
23. Waugh, R. W., Buted, R. R. The zero bias schottky diode detector at temperature

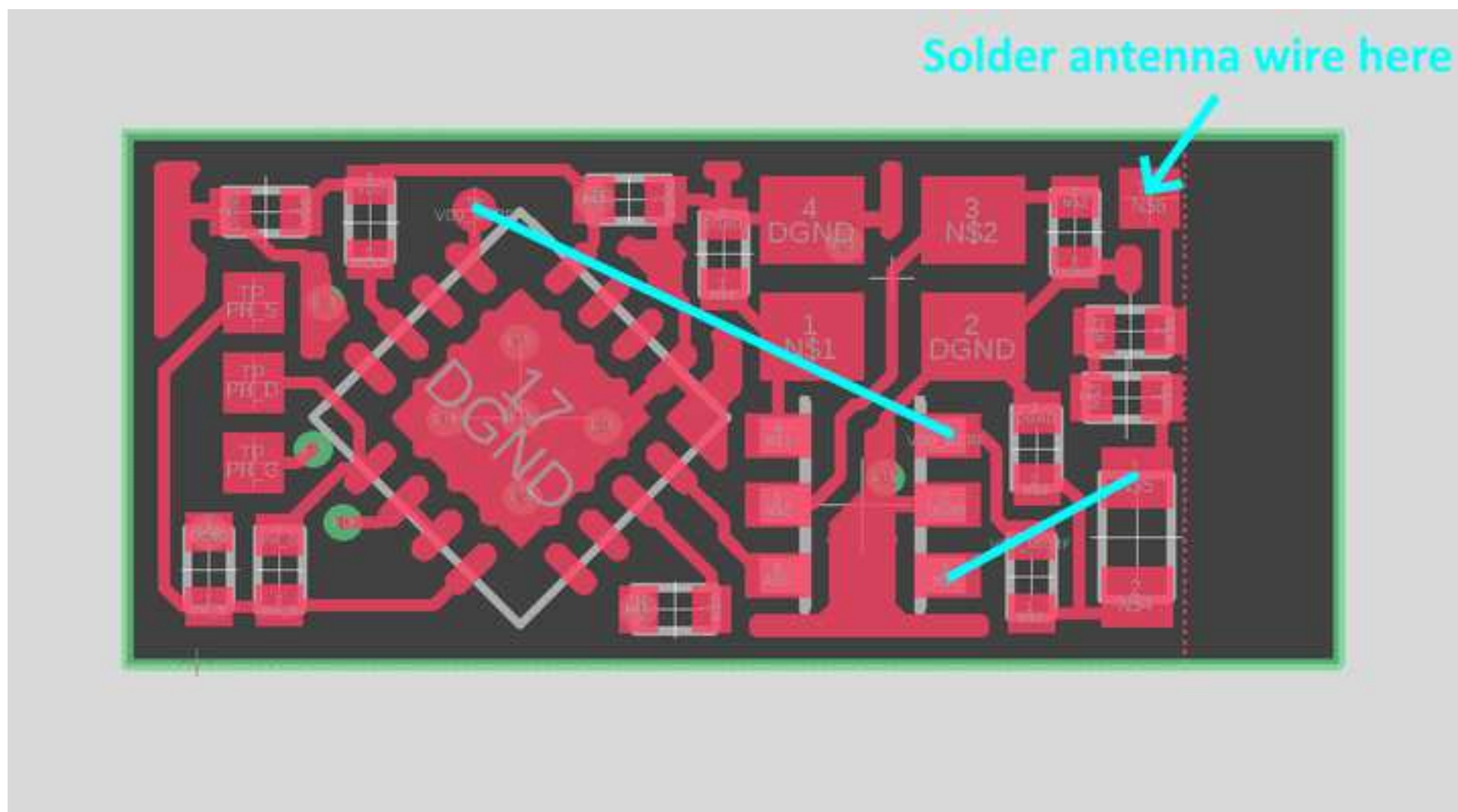
661 extremes-problems and solutions. *Proceedings of the WIRELESS Symposium*. 175–183 (1996).
662 24. Satoh, Y., Ikata, O., Miyashita, T. RF SAW filters at <[http://www.te.chiba-](http://www.te.chiba-u.jp/lab/ken/Symp/Symp2001/PAPER/SATOH.PDF)
663 [u.jp/lab/ken/Symp/Symp2001/PAPER/SATOH.PDF](http://www.te.chiba-u.jp/lab/ken/Symp/Symp2001/PAPER/SATOH.PDF)> (2011)
664 25. Soffer, E. Effect of electrical stimulation of the lower esophageal sphincter in
665 gastroesophageal reflux disease patients refractory to proton pump inhibitors. *World Journal of*
666 *Gastrointestinal Pharmacology and Therapeutics*. **7** (1), 145 (2016).
667 26. Microsemi ZL70323 MICS-band RF miniaturized standard implant module (MiniSIM).
668 (July), at <[https://www.microsemi.com/document-portal/doc_download/135307-zl70323-](https://www.microsemi.com/document-portal/doc_download/135307-zl70323-datasheet)
669 [datasheet](https://www.microsemi.com/document-portal/doc_download/135307-zl70323-datasheet)> (2015).
670

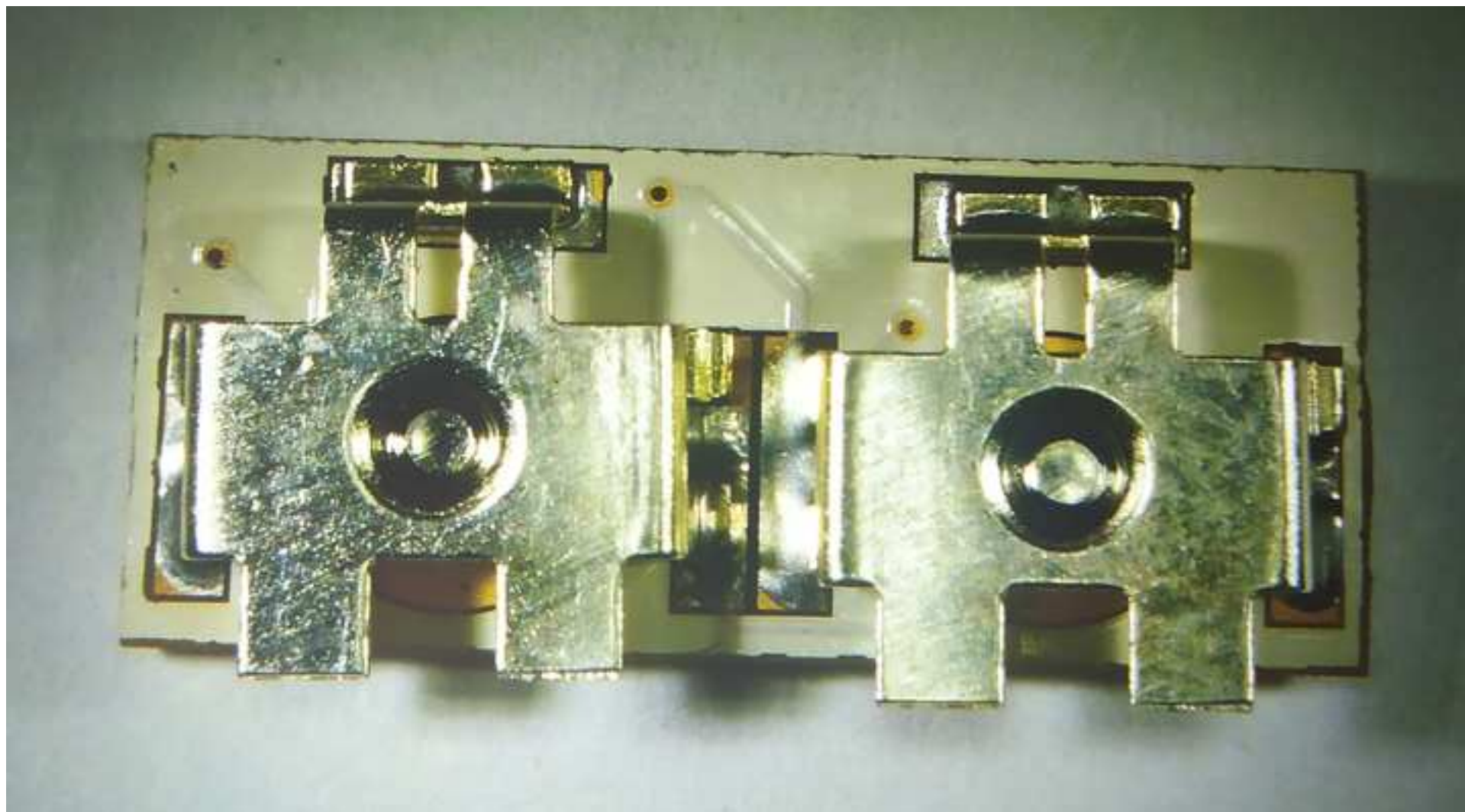


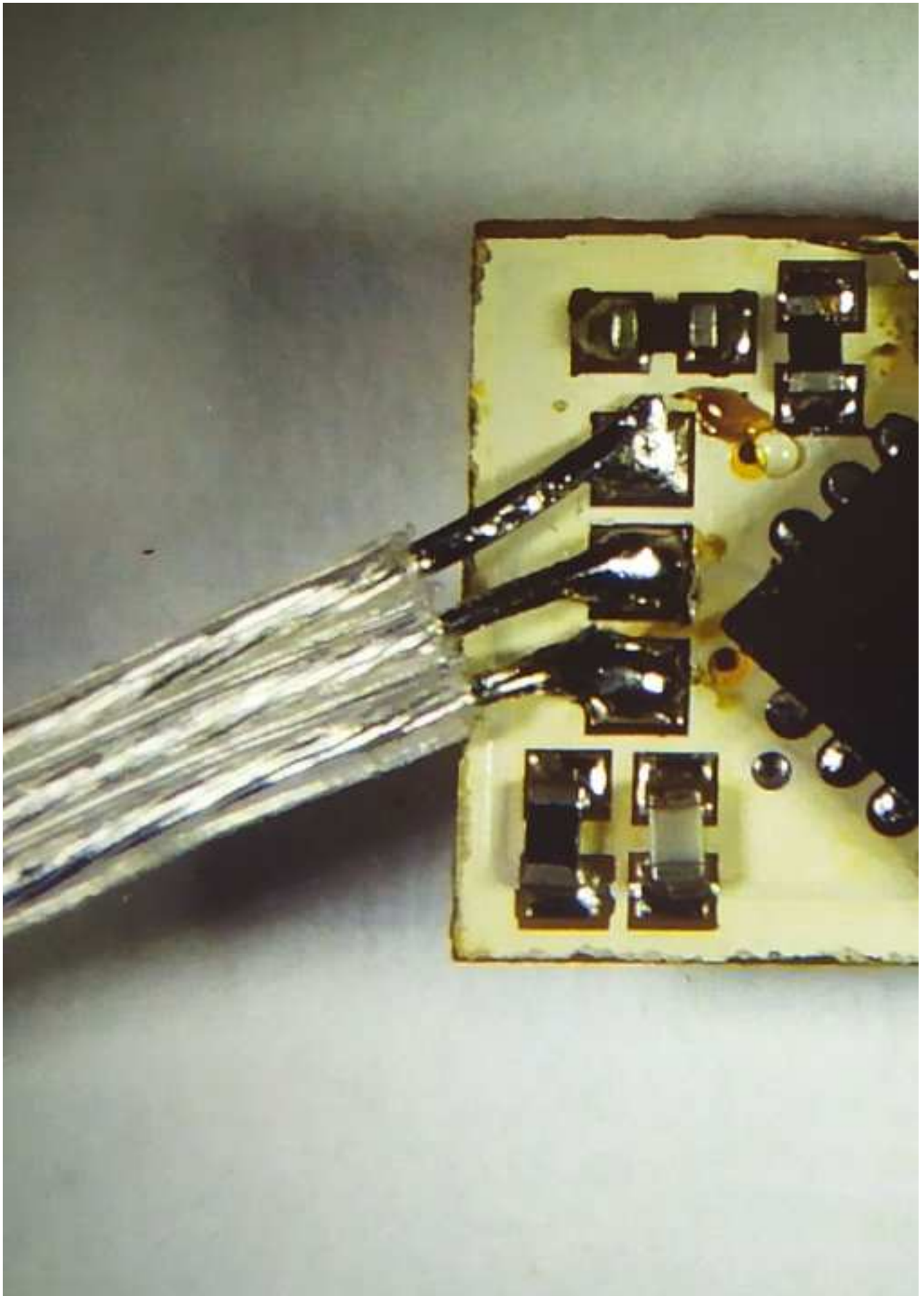


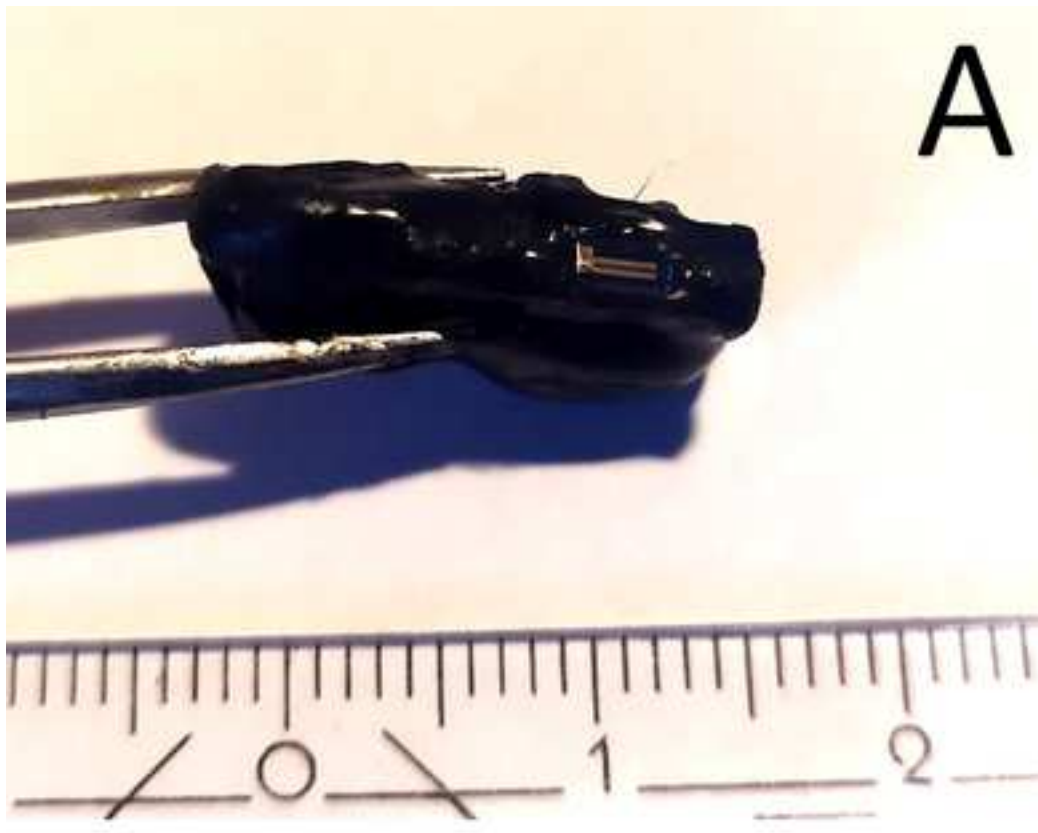


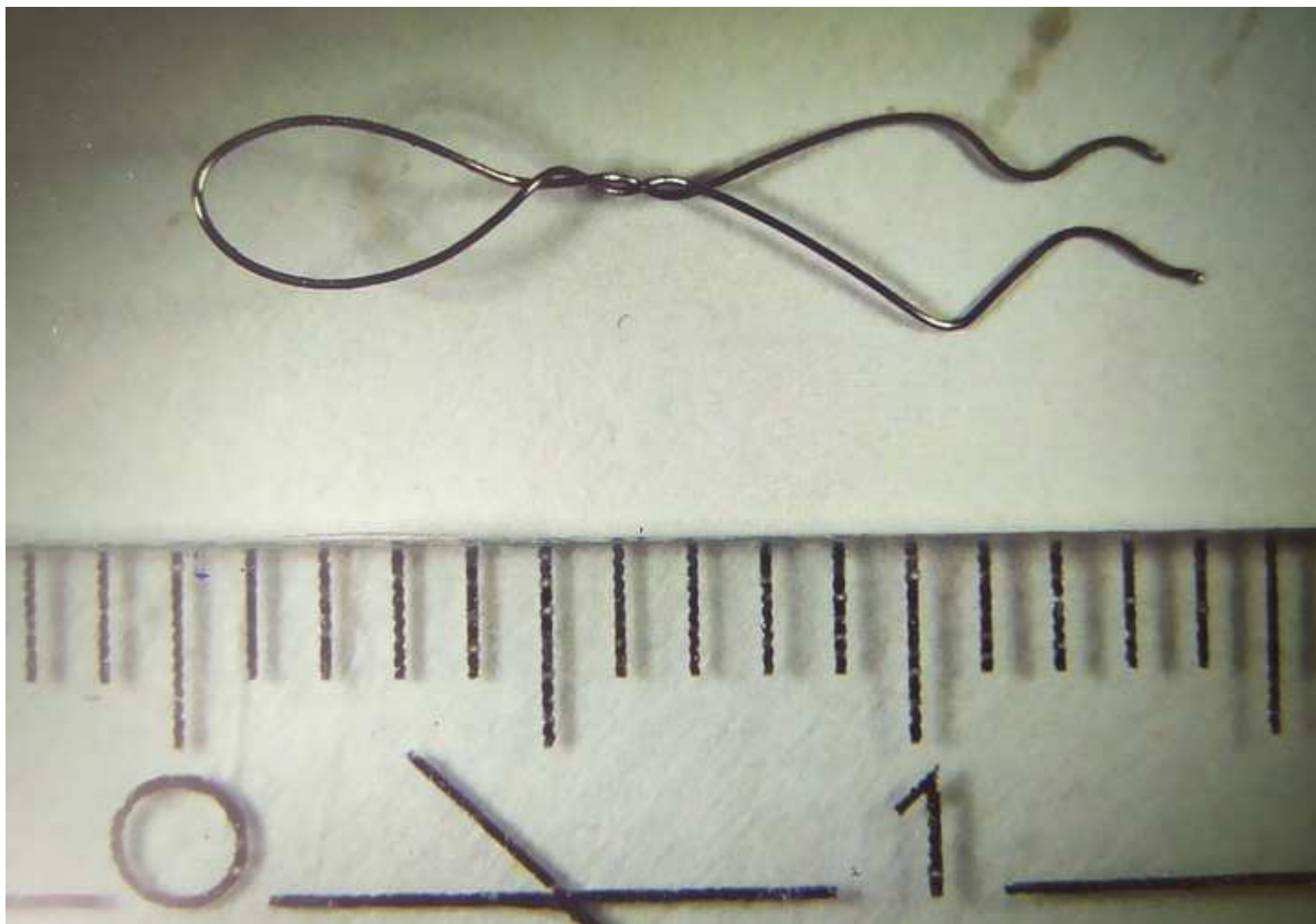




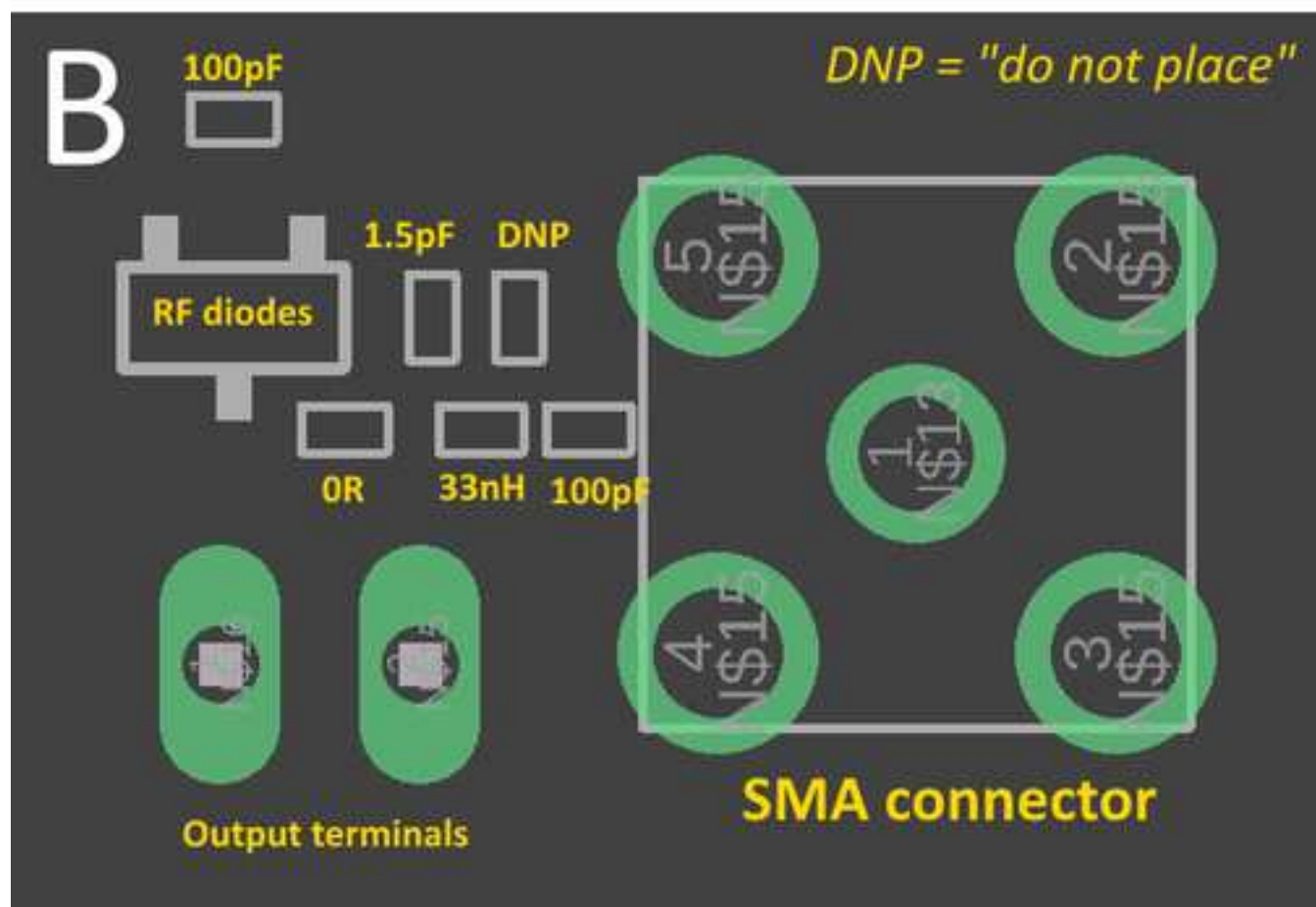
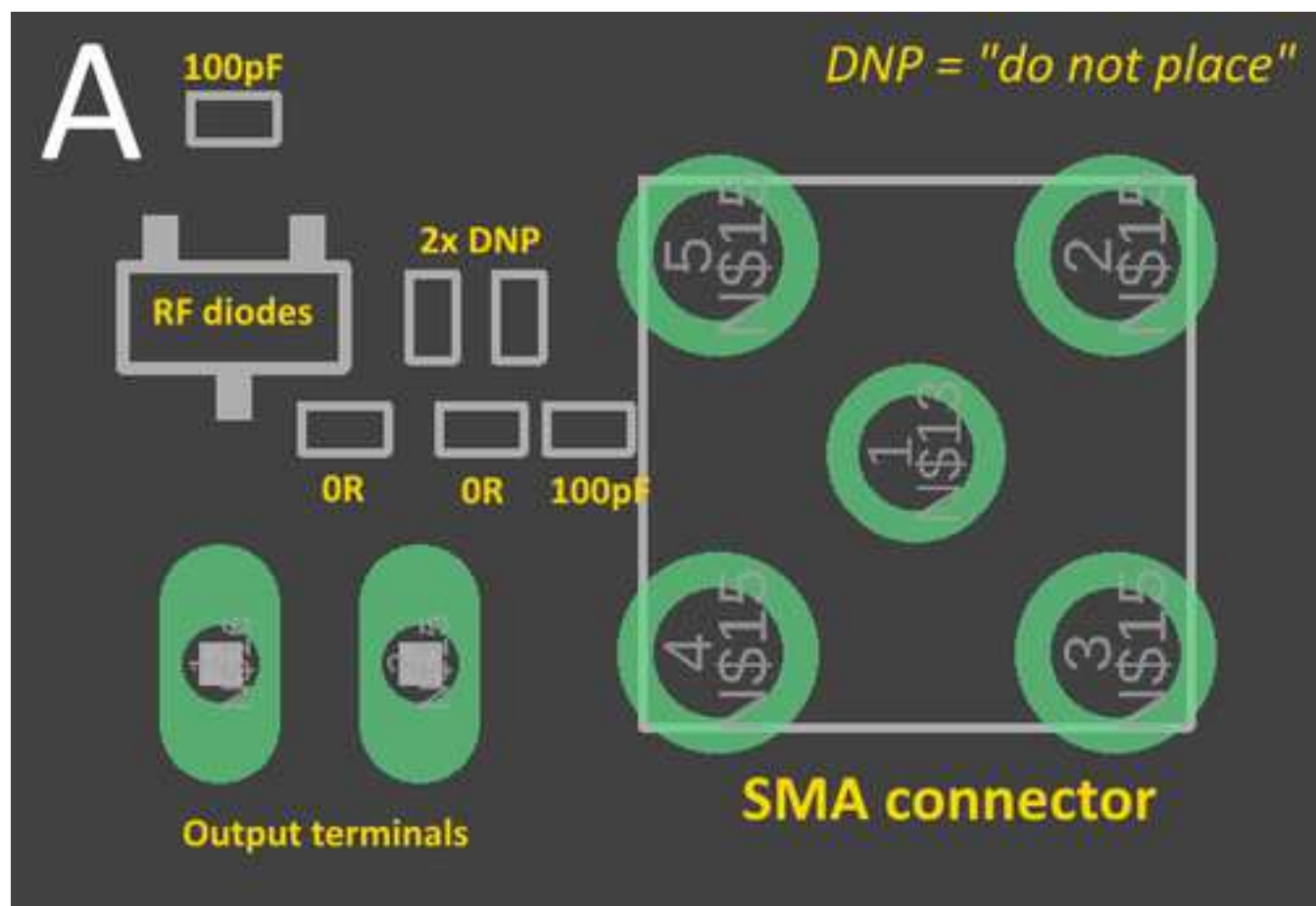


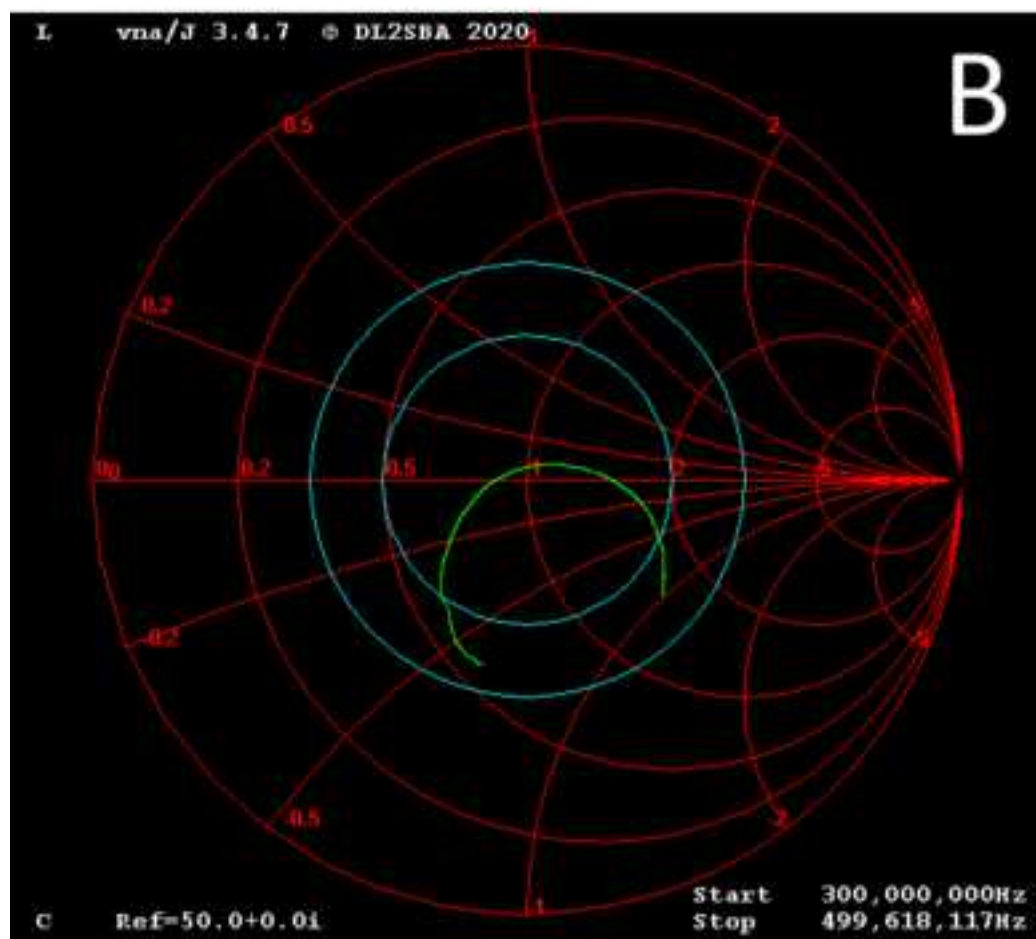
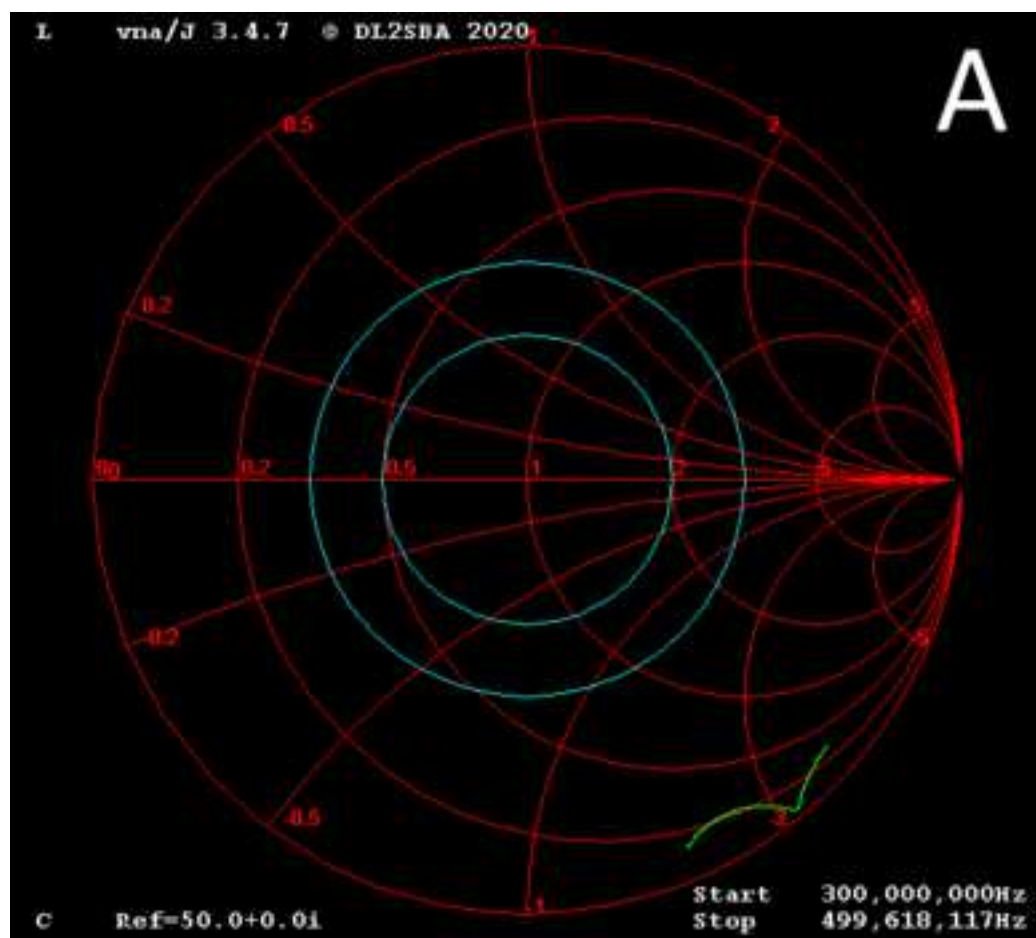




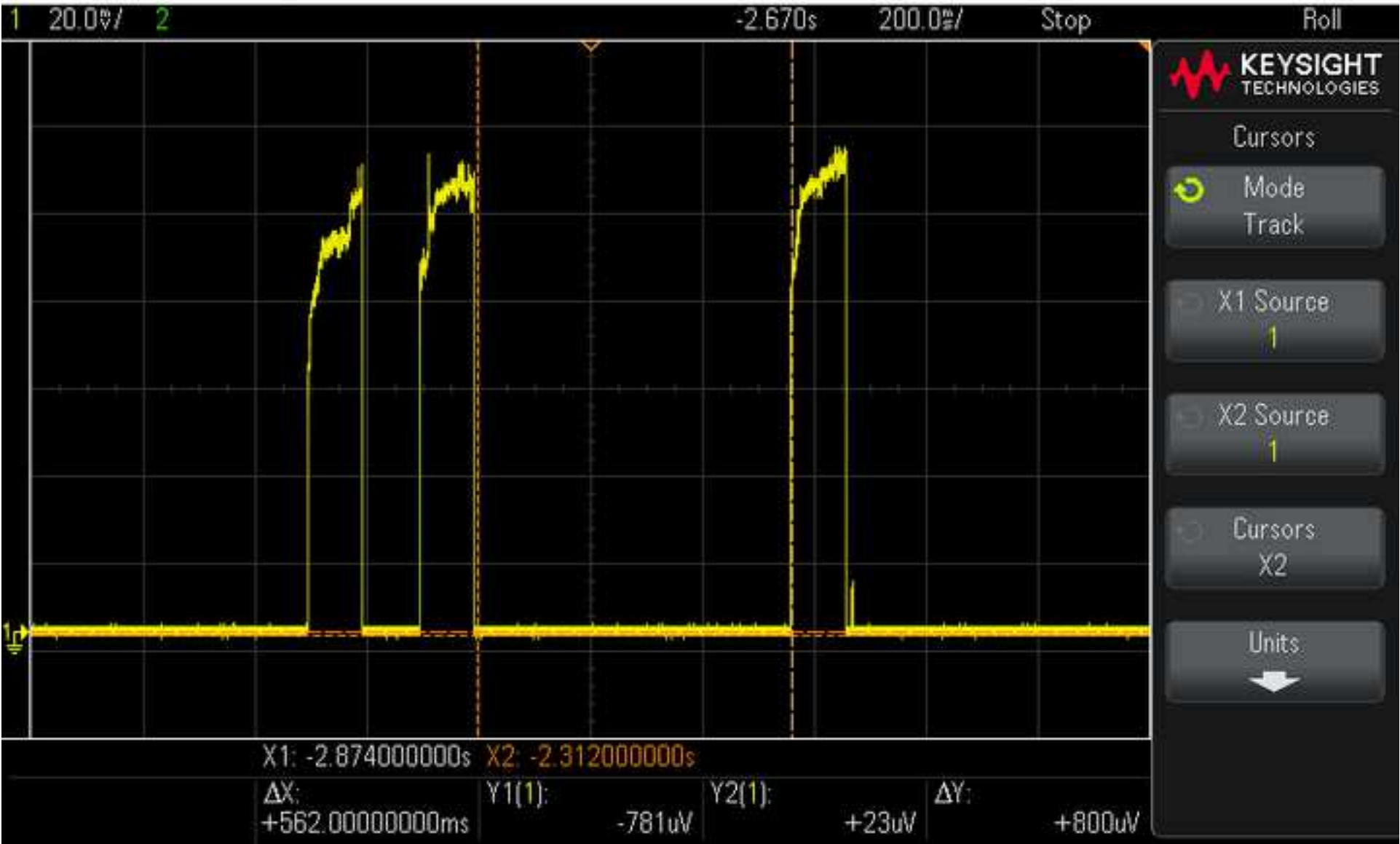


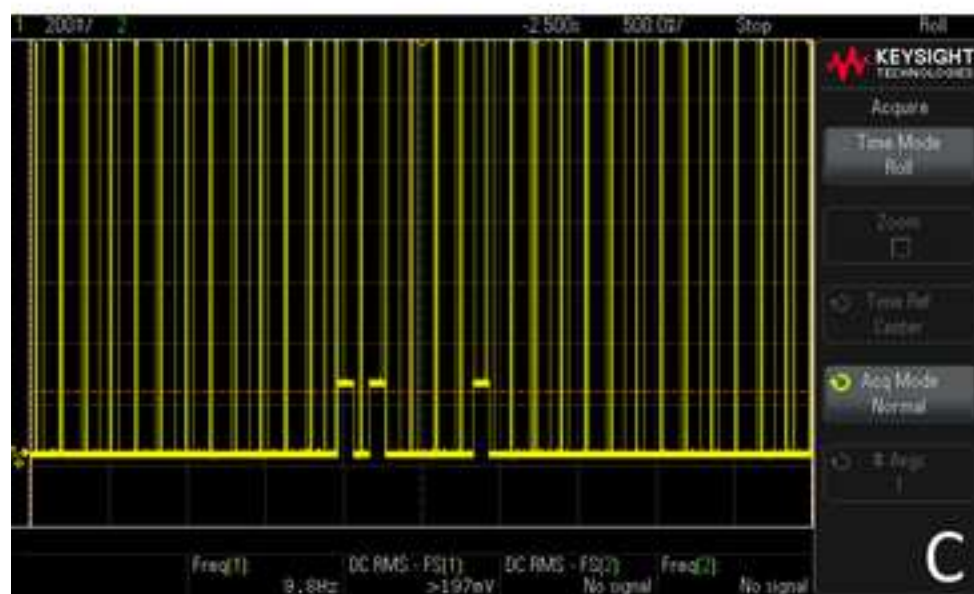
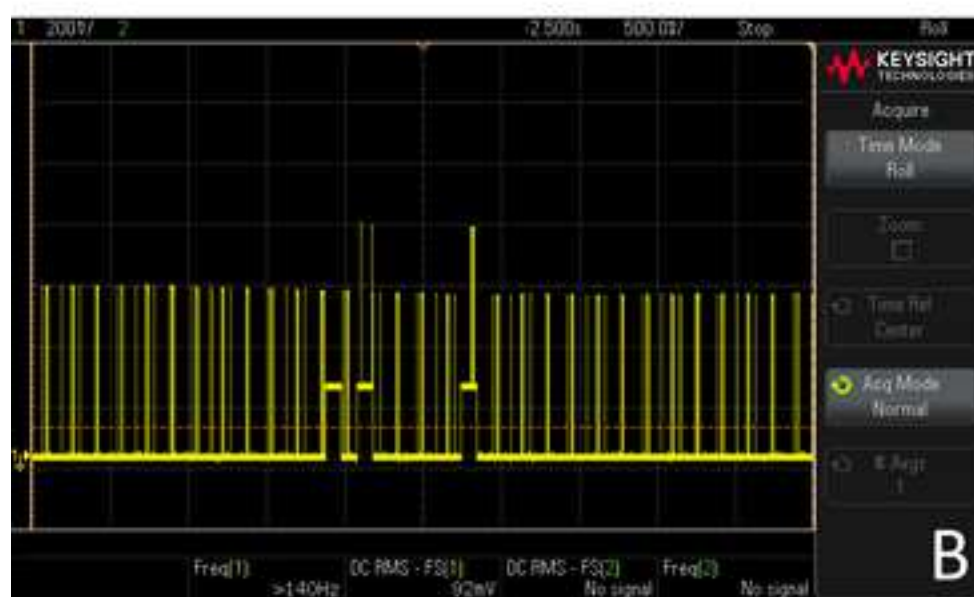


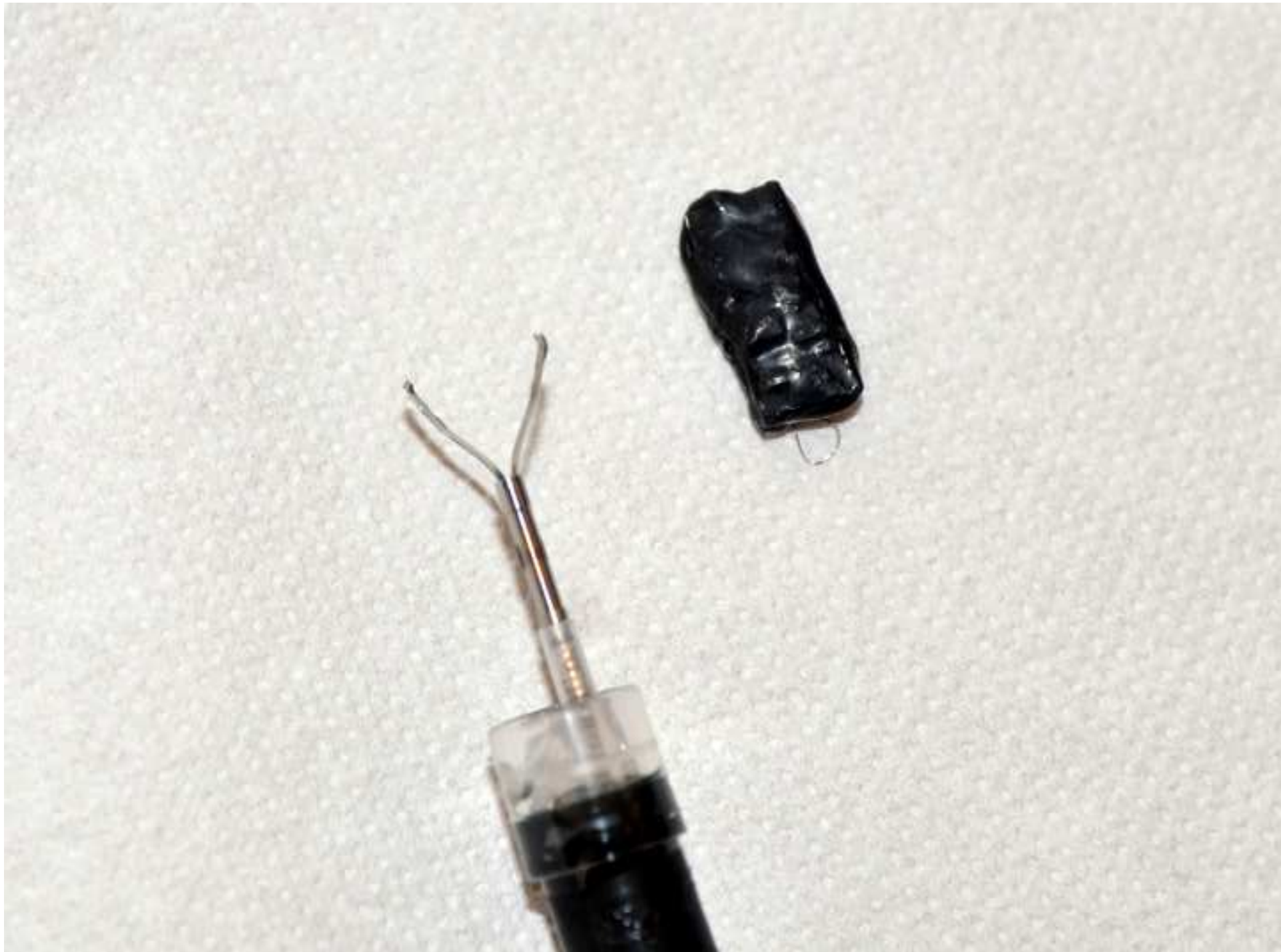


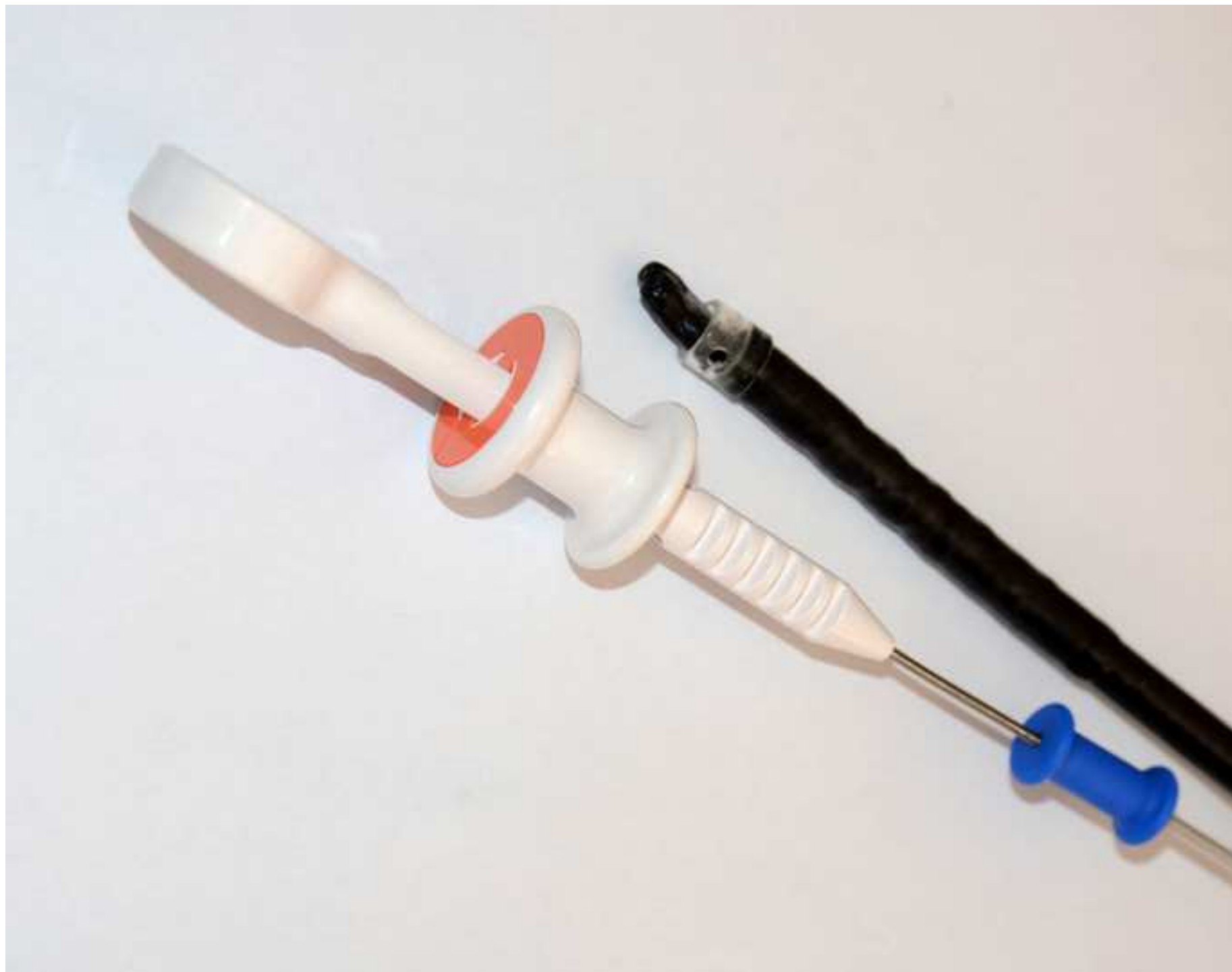


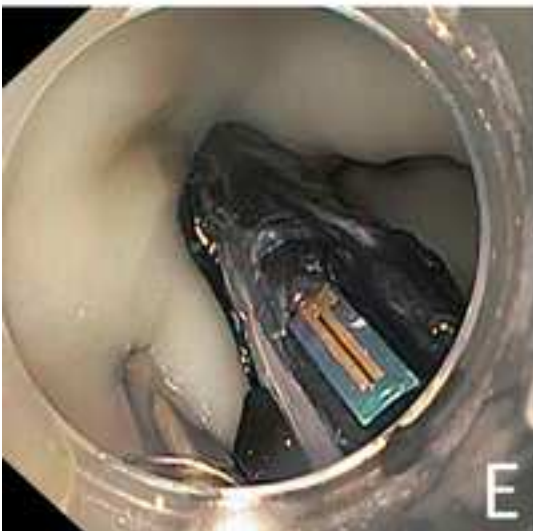
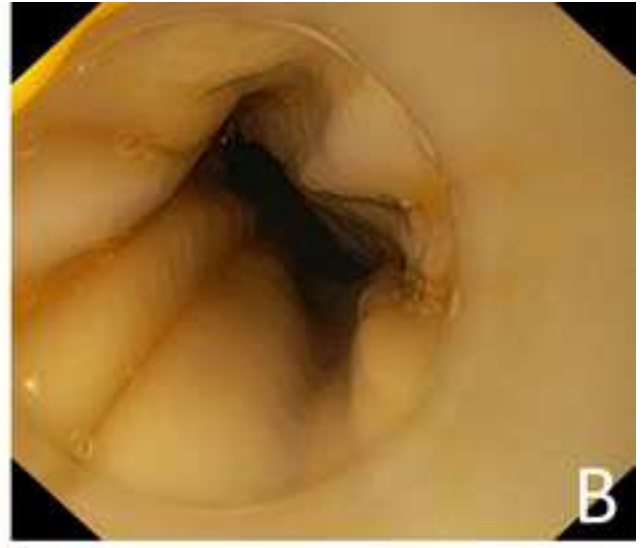
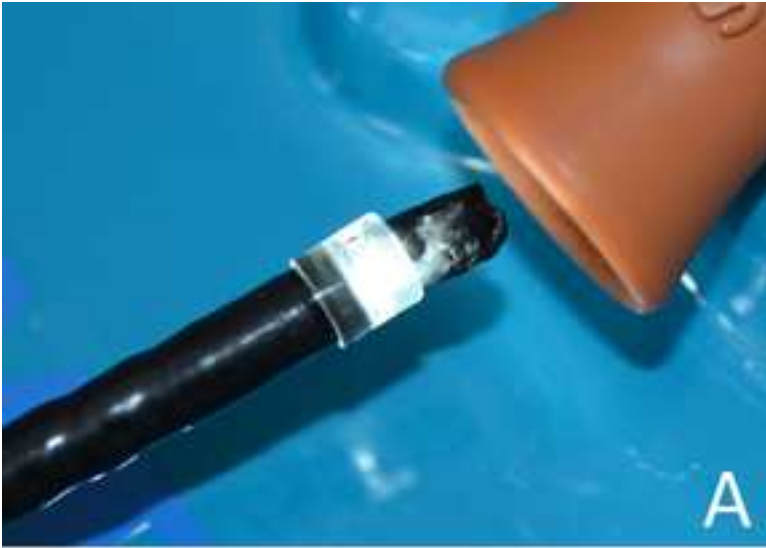
EDU-X 1002A, CN56390176: Mon Jul 12 14:38:30 2021



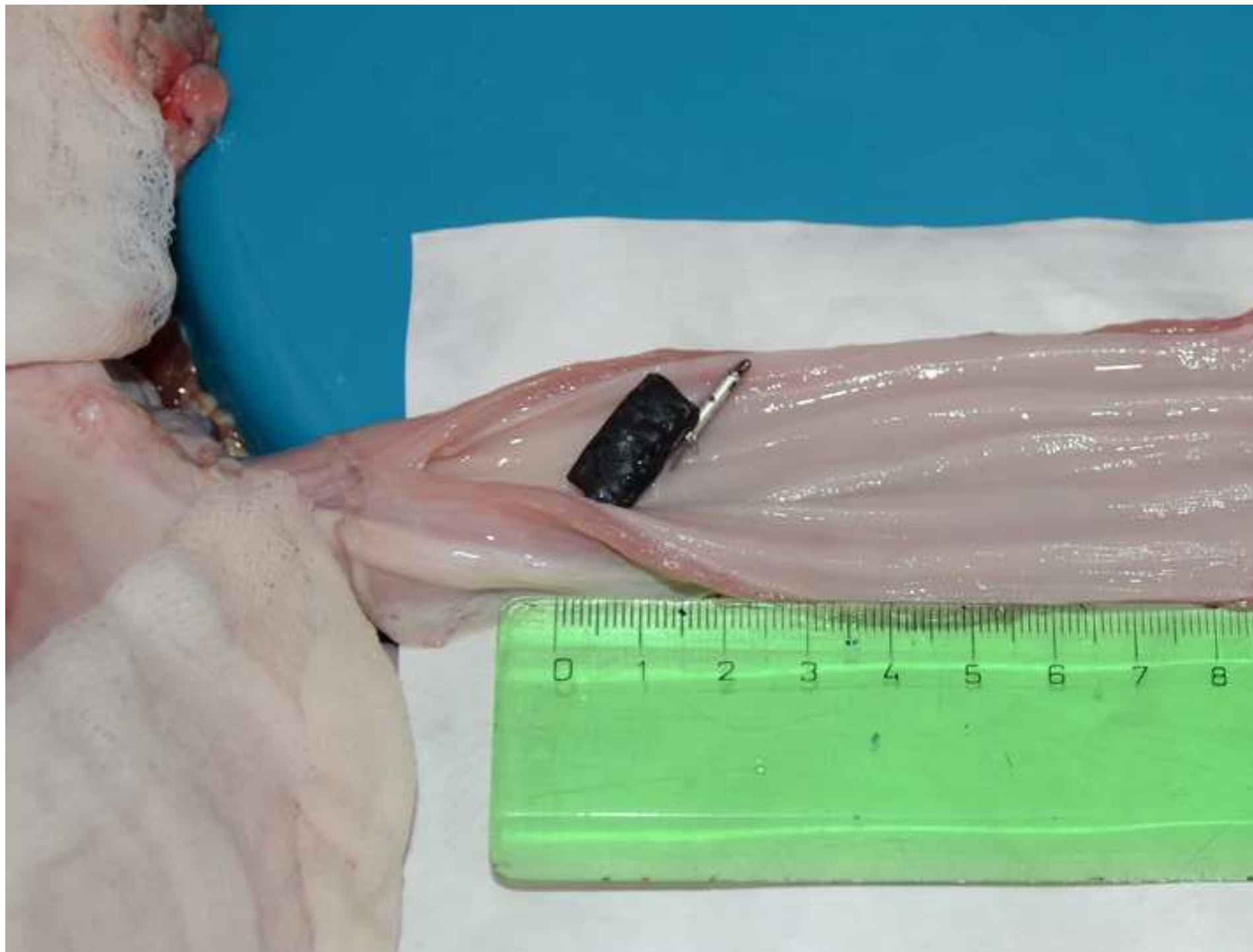












		Calibration data	
pH value (cal. meter) [-]	Pulse length [ms]	Calc. volt. output [mV]	
3.98		400	1200
10.01		710	1510

Measured data			
pH value (cal. meter) [-]	Calc. volt. output [mV]	Estimated pH [-]	
0.62	1010	0.28	
3.98	1200	3.98	
10.01	1490	9.62	
0.62	1020	0.48	
7.01	1350	6.90	
3.98	1220	4.37	
10.01	1480	9.43	
3.98	1210	4.17	
7.01	1350	6.90	
Std. deviation of pH [-]			
Mean error [-]			

Error [abs. pH]

Error [%]

-0.34 -54%

0.00 0%

-0.39 -4%

-0.14 -23%

-0.11 -2%

0.39 10%

-0.58 -6%

0.19 5%

-0.11 -2%

0.30

0.25

Measured data			
pH value (cal. meter) [-]	Calc. volt. output [mV]	Estimated pH [-]	
0.62	1010		0.28
3.98	1220		4.37
7.01	1340		6.70
10.01	1520		10.20
Std. deviation of pH [-]			
Mean error [-]			

Error [abs. pH]	Error [%]	
-0.34	-54%	
0.39	10%	
-0.31	-4%	
0.19	2%	
0.36		
0.31		



Click here to access/download

Table of Materials

JoVE_Materials-62864R1.xls



18th July 2021

Dear Editor,

On behalf of the author team, let me thank you and the reviewers for providing valuable feedback for our article. Please find our comments and corrective actions towards all comments and recommendations of you and the reviewers on the following pages of this letter. The questions / recommendations of the reviewers are underlined, while our answers are in plain text. We also enclose the modified manuscript with highlighted changes (by using the Track changes function of Microsoft Word) and modified figures + the Materials and equipment list.

Thank you for considering our manuscript for publication in the Journal of Visualized Experiments.

Yours sincerely,

Marek Novák (also on behalf of the co-authors).

Editorial Changes

Editor's comment: 1. Please take this opportunity to thoroughly proofread the manuscript to ensure that there are no spelling or grammar issues.

Our reply: The manuscript has been thoroughly read and mistakes caused by bad spelling or grammar were corrected.

Editor's comment: 2. Please provide an institutional email address for each author.

Our reply: This was added to the manuscript.

Editor's comment: 3. Please define the abbreviations before use (ISFET, PCB, FEB, etc.)

Our reply: This was edited, thank you for pointing it out.

Editor's comment: 4. JoVE cannot publish manuscripts containing commercial language. This includes trademark symbols (TM), registered symbols (®), and company names before an instrument or reagent. Please remove all commercial language from your manuscript and use generic terms instead. All commercial products should be sufficiently referenced in the Table of Materials.

Our reply: We checked the manuscript and all commercial information should be strictly in the Table of Materials.

Editor's comment: 5. Please include an ethics statement before your numbered protocol steps, indicating that the protocol follows the animal care guidelines of your institution.

Our reply: Our method does not involve living animals. The stomach and esophagus were purchased from a local butchery as their standard product. This procedure is in accordance with Czech laws and we prefer it because of the "3R" principle (Replacement, Reduction and Refinement). We find it unethical to use a dedicated experimental animal only for the purpose of organ harvesting when another legal method which saves the animal is available.

Editor's comment: 6. Please note that your protocol will be used to generate the script for the video and must contain everything that you would like shown in the video. Please add more details to your protocol steps. Please ensure you answer the "how" question, i.e., how is the step performed? Alternatively, add references to published material specifying how to perform the protocol action. Please add more specific details (e.g. button clicks for software actions, numerical values for settings, etc) to your protocol steps. There should be enough detail in each step to supplement the actions seen in the video so that viewers can easily replicate the protocol.

Our reply: Changes to some steps (e.g. 2.5. and 3.6.s) were made to improve cohesion and provide more detailed information about the steps. We omitted the step 4.3. from the protocol as it is not directly related to the procedure, it only checks whether the step 4.2. was done correctly.

Editor's comment: 7. For time units, please use abbreviated forms for durations of less than one day when the unit is preceded by a numeral throughout the protocol. Do not abbreviate day, week, month, and year. Examples: 5 h, 10 min, 100 s, 8 days, 10 weeks

Our reply: The manuscript was corrected.

Editor's comment: 8. For SI units, please use standard abbreviations when the unit is preceded by a numeral throughout the protocol. Abbreviate liters to L to avoid confusion. Examples: 10 mL, 8 μ L, 7 cm²

Our reply: The manuscript was corrected.

Editor's comment: 9. Being a video-based journal, JoVE authors must be very specific when it comes to the humane treatment of animals. Regarding animal treatment in the protocol, please add the following information to the text:

- a) Please include an ethics statement before all of the numbered protocol steps indicating that the protocol follows the animal care guidelines of your institution.
- b) Please mention how animals are anesthetized and how proper anesthetization is confirmed.
- c) Please specify the use of vet ointment on eyes to prevent dryness while under anesthesia.
- d) For survival strategies, discuss post-surgical treatment of animal, including recovery conditions and treatment for post-surgical pain.
- e) Discuss maintenance of sterile conditions during survival surgery.
- f) Please specify that the animal is not left unattended until it has regained sufficient consciousness to maintain sternal recumbency.
- g) Please specify that the animal that has undergone surgery is not returned to the company of other animals until fully recovered.
- h) Please do not highlight any steps describing euthanasia.

Our reply: This is not applicable – the method does not involve living animal experiments.

Editor's comment: 10. Please ensure that the highlighted steps form a cohesive narrative with a logical flow from one highlighted step to the next. Please highlight complete sentences (not parts of sentences). Please ensure that the highlighted part of the step includes at least one action that is written in the imperative tense.

Our reply: We checked the steps and are of an impression that the protocol is following these instructions. We are, however, open to any recommendations from you side.

Editor's comment: 11. Please ensure that the Discussion explicitly covers the following with citations:

- a) Critical steps within the protocol
- b) Any modifications and troubleshooting of the technique
- c) Any limitations of the technique
- d) The significance with respect to existing methods
- e) Any future applications of the technique

Our reply: The section was written to discuss all these topics. We are welcome to any further changes if these will be required.

Editor's comment: 12. Please consider combining some figures together to form a multipaneled single figure. Ensure to label the figures to make them more informative.

Our reply: We agree, multiple figures were combined.

Editor's comment: 13. Please sort the Table of Materials in alphabetical order.

Our reply: This was done – we created several “categories” of the material (according to the specific step they are connected to) and sorted them in alphabetical order. If requested, we can sort everything as a single table but we suggest keeping several sub-tables for clarity.

Reviewer 1

Reviewers's summary: This manuscript describes the fabrication, bench, and ex vivo testing of an implantable wireless pH sensor and passive receiver. It is interesting and would have value for others working in the field of biomedical engineering. In general, the protocol steps are well written and clear, but there are some steps that are very superficially described, and some essential background information is not given. I was also surprised at the lack of schematics or description of the electronic design - this would probably be more valuable than the clinical background for a methods paper. Materials are well described, but the equipment used should be more detailed. The representative results were reasonable, and it was good to see both in vitro and ex vivo data reported. Calculation of sensor error was performed using an unusual method - taking only the standard deviation of the absolute errors. This will give a measure of dispersion of error, but not its magnitude. This should be changed to the mean error (with SD quoted alongside). In the discussion, it would be useful to describe in more detail how other receivers could be used to collect data from the device. This would make the paper more generalisable and useful, as the passive receiver described is quite specific to this application. The code accompanying the paper is well commented, and it would be easy to understand and adapt.

Our reply: According to your summary, some of the steps which were described only briefly were expanded and the use of various instruments was described in more detail or the procedure was cited (e.g. step 2.8 and 2.9). The mean error was added alongside the standard deviation of absolute error to make the statistical analysis of the results clearer. Other types of receivers and specific settings which will lead to successful data reception are now discussed in the manuscript. The schematic diagram was embedded as a Supplementary material and the design of the circuit is now described in the Introduction.

Reviewers's comment: Abstract: Currently written in the style of "reporting research", should be adapted to make clear it is describing a method. GERD should be defined.

Our reply: The abstract was modified to better fit the nature of the article.

Reviewers's comment: Introduction: How does neurostimulation work? What is the principle-of-operation of an ISFET, and why would it be chosen as a pH sensor for implantable devices? Which animal model have you chosen, and why is it a good model?

Our reply: The introduction section was expanded with the citations of current literature in terms of neurostimulation treatment. The principle of operation of an ISFET sensor as well as its suitability for implantable devices was mentioned. The chosen animal model represents the anatomy of a human body in terms of size and structure. This was also mentioned in the Introduction.

Reviewers's comment: 1.3 Define FEP

Our reply: Added to the manuscript.

Reviewers's comment: 1.8 How does black epoxy enable later inspection? Surely transparent epoxy would be better?

Our reply: A thorough inspection of the PCB is done before encapsulation. The reason for inspection is to ensure that no metallic component or PCB is exposed to the environment, and everything is covered with epoxy. Thus, black or colored opaque epoxy provides a better way to inspect possible voids in the epoxy layer. We acknowledge the fact that the explanation was not clear enough so we decided to provide a more detailed explanation within the step.

Reviewers's comment: 2 + 3: Schematic diagrams should be included for the circuits

Our reply: A schematic diagram for the electronics part (microcontroller + RF transmitter) was added as a Supplementary file (as it is not strictly required to reproduce the device as described in the procedure). As for the zero-bias Schottky receiver, the PCB was drawn directly without the schematic diagram. We think that due to a simple design (matching network, 2 diodes, and output capacitor), the circuit can be very easily decoded by a reader with experience in electronics circuit design.

Reviewers's comment: 2.3 Include orientation of polarised components (e.g. the microcontroller) on the PCB for figure 3.

Our reply: The pin 1 markings (previously grey) were changed to red color and the figure title was changed to make the orientation more clear. The crystal is not a polarised component.

Reviewers's comment: 2.4 Describe what equipment used to heat PCB, and timings.

Our reply: The hot air gun model was added to the Materials section. The temperature profile which was used was added to the manuscript.

Reviewers's comment: 2.9 State which programmer used to programme microcontroller

Our reply: Microchip PICkit 3 – it was added to the Material and equipment list.

Reviewers's comment: 2.10 What material is used for the antenna?

Our reply: SWG38 copper wire with transparent enamel coating – the type was added to the Material and equipment list.

Reviewers's comment: 2.14 Make clear why a 24h delay is introduced. Can initial testing of the completed device be performed before encapsulation to check function?

Our reply: The 24-hour delay is introduced for the epoxy to thoroughly cure (which takes at least several hours according to the epoxy datasheet) and for comfortable reproduction of the procedure. In our case, the lab for manufacturing the electronics is located far from the experimental endoscopic lab (around 180 km). Thus, the delay is needed for transportation of the finished pH sensors from one site to the other. Usually, the sensors were manufactured a day before the experimental implantation and one of the team members traveled with them in the evening before implantation. The delay can be altered in the source code very easily by modifying the delay. A short paragraph discussing this was added to the Discussion.

Thank you for recommending providing a procedure to check the sensor before encapsulation. We created another firmware without the 24-hour delay and altered the manuscript accordingly.

Reviewers's comment: 2.16 How is the epoxy applied?

Our reply: The same way as the pH sensor – syringe with a needle – the protocol was altered to provide this information to the reader.

Reviewers's comment: 2.18 Reference Fig 11

Our reply: Thanks for spotting the mistake – added to the manuscript.

Reviewers's comment: 3.2 Are both Fig 12 + 13 necessary? Would one be enough?

Our reply: The figures describe two different setups – one for matching and another for use as a receiver. Originally, we tried to make one picture (not multi paneled), however, there was too much text packed in a very small area which affected the conciseness of the figure. For this reason, we provided a multipanel figure (now Fig. 11) instead of two separate figures.

Reviewers's comment: 3.5 State which vector network analyser is used, and necessary specifications

Our reply: Added to the Materials and equipment list.

Reviewers's comment: 3.6 Explain how the values of the matching components can be calculated

Our reply: A freeware software from Iowa Hills software (<http://www.iowahills.com/9SmithChartPage.html>) was recommended in the protocol. In practice, the impedance matching components are rarely calculated by hand.

Reviewers's comment: 4.1 Change to Fig 16/17

Our reply: Fixed, thank you.

Reviewers's comment: 4.2 State the source of the pH buffers

Our reply: The buffers were prepared on-site according to standard laboratory procedures and subsequently verified with a laboratory pH meter. The type of the buffers was added to the step.

Reviewers's comment: 4.4 I can only see three pulses, not four? Amend Fig 16/17 screen capture to show more clearly which time is being measured.

Our reply: Four pulses were used in the previous version of the firmware, the text was corrected. As for the amendment of Fig 16/17, the measured time is shown by on-screen cursors (two orange vertical dashed lines). Is it necessary to provide another visual clue for the reader?

Reviewers's comment: 5. Provide more detail on the ex vivo animal model - source, animal size/age, how dissection was performed.

Our reply: No living animal model was used, a pig stomach with the esophagus (weight of animal of around 40-50 kg) was purchased from a local pig farm as it is a consistently offered item. The animal from which the stomach and esophagus were obtained was not dedicated for the experiment. The clarification was added to the Materials and equipment list.

Reviewers's comment: 5.2 Should be Figs 18-20

Our reply: Fixed, thank you.

Reviewers's comment: 5.5 How is the sensor attached to the esophageal wall?

Our reply: The description of the sensor implantation was clarified.

Reviewers's comment: 6.2 Describe in more detail how solutions were injected into the esophagus. What volume? How did you ensure the previous solution was removed?

Our reply: This was clarified in the manuscript. A wash with 100 ml of DI water was introduced between injections. The volume of each solution was also added.

Reviewers's comment: Line 309: between the end of the second pulse and what?

Our reply: Fixed, thank you – between the end of the second pulse and the beginning of the third pulse.

Reviewers's comment: Line 316: report the error mean \pm SD, not just the SD of the errors

Our reply: \pm SD as well as the error mean was added.

Reviewers's comment: Line 328: Table 4 is not needed, a text description of the effect is sufficient

Our reply: We agree, the table was removed.

Reviewers's comment: Discussion: Describe in more detail how other receivers could be used to measure the output from the implanted sensor.

Our reply: The possible use of a spectrum analyzer or even a common heterodyne receiver was described in more detail, including the pros and cons.

Reviewer #2:

Reviewer's comment: * Specify the advantage of this battery-powered pH sensor over wirelessly powered battery-less implantable pH sensor.

Our reply: This topic was addressed in the discussion section.

Reviewer's comment: * The authors have shown the change in output due to mobile interference in 15 cm proximity. I suggest the authors show the effect of interference in further close proximity.

Our reply: After submitting the paper for peer review, we spotted a fault in the used equipment – the antenna which is connected to the passive receiver was faulty (short-circuit at the connector). The output voltage of the passive receiver seemed quite low but we attributed this to the small size of the transmitting antenna and its proximity to metallic parts (mainly batteries). We replaced the antenna, did the measurements again and we got a much stronger response from the sensor. As a result, we revised this part of the manuscript. It was shown that the GSM signal injects strong peaks to the signal but due to chosen ASK modulation scheme of the sensor, these can be easily filtered out by rejecting the high-frequency component of the signal with a passive filter.

Reviewer's comment: * The authors have specified a limit of 10 cm proximity for the receiver from the sensor. I suggest the author show the variance in the output and the incurred error with the change in the proximity of the receiver from the implanted sensor.

Our reply: The measurement on now Fig. 13 was re-done at 20 cm which is well beyond the range between the transmitter and receiver when using it as intended (communication between the pH sensor and an implantable neurostimulator, both in the proximity of a lower esophageal sphincter). During the GSM interference test, the distance was 10 cm. Rather than incurring errors to the transmitted data, the signal will be indistinguishable from the noise and surrounding RF transmitters.

As the antennas are close to each other during all experiments, wireless communication happens in a near-field. Thus, equations and models which are usually used (i.e. free space path loss) do not work and even small variances in the angular position of the antennas and construction may lead to drastically different outcomes. Our opinion is that showing two distinct data points (10 cm and 20 cm) gives sufficient information about the expected performance.

Reviewer's comment: * The authors have used an AG1 battery. I suggest the authors to mention what kind of modifications are required to incorporate other types of batteries.

Our reply: This was added to the discussion. Generally, silver oxide/alkaline/carbon-zinc batteries provide better performance and simplify the circuit than using primary lithium

batteries or Li-Ion batteries. Small primary lithium batteries have high internal resistance which would cause significant voltage drops, potentially leading to the brown-out of the microcontroller and RF transmitter during normal operation. Lithium-ion batteries, on the other hand, are incompatible with 3.3 V microcontrollers (the operating voltage of Li-Ion batteries is around 3.0 V to 4.2 V), adding complexity to the circuitry (requirement of a regulator or DC/DC step-down converter). Two primary 1.5 V button cells are the best commonly found type of battery based on the availability, operating voltage, and internal resistance.

Reviewer's comment:* I request the authors to specify whether the used commercial ISFET pH sensor offers higher sensitivity compared to other sensors available.

Our reply: The sensitivity of ISFET pH sensors (and pH sensors in general) usually follows the Nernst equation if the circuit is designed properly. In this system, the sensor exhibited almost ideal Nernst response of around -51.7 mV/pH (Nernst equation gives an ideal slope of -58 mV/pH for 25 °C). Thus, its sensitivity is almost on par with traditional glass electrodes and better than reported values for antimony pH sensors (-45 mV/pH [1]).

[1] [https://www.annalsthoracicsurgery.org/article/S0003-4975\(10\)60791-6/pdf](https://www.annalsthoracicsurgery.org/article/S0003-4975(10)60791-6/pdf)

Reviewer's comment:* Demonstration of removal of faulty soldering and redoing the soldering would help the readers.

Our reply: The assembly of the printed circuit board with miniature 0402 components and a small-pitch QFN package requires a certain level of skill and prior experience. All components are temperature and ESD sensitive, so we advise that the procedure of manufacturing of the ISFET pH sensor assembly and the electronics is performed only by a person with prior experience in the assembly of printed circuit boards. While a guide for de-soldering of the components and SMT rework could be helpful for some readers, creating a comprehensive and useful guide with visual demonstrations would most likely disrupt the cohesion of the article/method. However, if the request to provide a de-soldering guide persists, we will be glad to provide it to the article.

Reviewer's comment:* In 1.3, mention the model number for the open-short circuit tester.

Our reply: It was added to the Material and equipment list.

Reviewer's comment:* In 1.4, mention whether the soldering needs to be dried before cleansing. If so, how much time for drying.

Our reply: Sonication or chemical treatment of bare dies is generally not recommended as it can disrupt the rather delicate internal structure which, in the case of a pH sensor, is fully exposed to the environment. Thus, it is advisable to skip the cleaning process for the ISFET sensor. We have added this information to the protocol.

Reviewer's comment:* In 1.5, mention the ratio of flux remover and water mixture used and the optimum range of the ultrasound power.

Our reply: The concentration of the flux remover solution and optimum range of ultrasound power was added to the manuscript.

Reviewer's comment:* In 1.11, specify the temperature is used by the authors in this method.

Our reply: This was added to the manuscript.

Reviewer's comment:* In 2.9, I recommend the authors to show the steps in programming the PCB using a microcontroller.

Our reply: Another article published in JoVE by us which describes this procedure in detail for the used PICkit 3 programmer was cited in the protocol. If a full explanation in the article is more suitable, we can add it based on the editor's opinion.

Reviewer's comment:* In 2.17, specify a list of materials that can be used in the place of titanium and mention why titanium is used.

Our reply: Step 2.17 was amended according to this comment.

Reviewer's comment:* In 4.1, I guess the output figure number is 16 and not 14.

Our reply: Yes, this is a mistake on our side, it was pointed out by another reviewer, too. It was fixed, thank you.

Reviewer's comment:* In 4.3, specify the pH meter used for calibration in the beaker test.

Our reply: The pH meter model was listed in the Material and equipment list.

Reviewer #3:

Reviewer's comment: 1. The authors used several abbreviated terms. For example, GERD and ASK modulated wireless output. Please introduce the full term prior to the abbreviation.

Our reply: Fixed, thank you for pointing this out.

Reviewer's comment: 2. The authors could consider giving a brief explanation in introduction section about the zero-bias Schottky diode-based receiver and ASK modulation. It will help readers from different fields to understand the principles and why specific wireless modulation module are chosen as a technical background.

Our reply: The introduction was altered according to this recommendation, thank you very much for it. The receiver only detects received power (often abbreviated as “RSS” – received signal strength). Thus, ASK modulation is the only viable modulation scheme. To detect other types of modulations (namely FSK and PSK), an active receiver is required.

Reviewer's comment: 3. In the protocol section 1, the authors could used epoxy to seal the electronics part. I wonder about the biocompatibility and the acid tolerance of the specific type of the epoxy

Our reply: For the initial experiments, we used automotive-grade epoxy because it was available at the time and was tested to successfully bond to FR-4 substrate in past. Depending on the nature of the experiment which will be done by the researcher, suitable epoxy (cost vs. performance) can be chosen. As we plan to proceed with experiments combining this sensor with a neurostimulator in a living animal, we conducted experiments with different epoxies during the peer-review of the article. Following this testing, we switched to Loctite Hysol EA M-31 CL medical-grade ISO 10993 compliant epoxy. The bond of the epoxy to FR-4 substrate was shown to be sufficient for encapsulation. The Materials and equipment list was altered accordingly as well as the discussion.

To enhance the biocompatibility for long-term implantation, further coating with a biocompatible material (i.e. parylene or Teflon) can be done. A short mention of this was also included in the manuscript. However, we think that a detailed description of the design of a long-term implantable device from the point of biocompatibility is outside of the scope of the article, and present literature from the material science field documents this topic well.

Note: Input data only into gre

1) Input calibration data			
pH value [-]	Pulse length [ms]		Calc. volt. output [mV]
	3.98	400	1200
	10.01	710	1510
2) Calculate pH based on the pulse length			
Pulse length [ms]	Calc. volt. output [mV]		Estimated pH [-]
	210	1010	0.28
	400	1200	3.98
	690	1490	9.62
	220	1020	0.48
	550	1350	6.90
	420	1220	4.37
	680	1480	9.43

open fields

a

use length

